Interpolation of parametric CNC machining path under confined jounce

Wei Fan, Xiao-Shan Gao, Wei Yan & Chun-Ming Yuan

The International Journal of Advanced Manufacturing Technology

ISSN 0268-3768
Volume 62
Combined 5-8

Int J Adv Manuf Technol (2012)
62:719-739
DOI 10.1007/s00170-011-3842-0

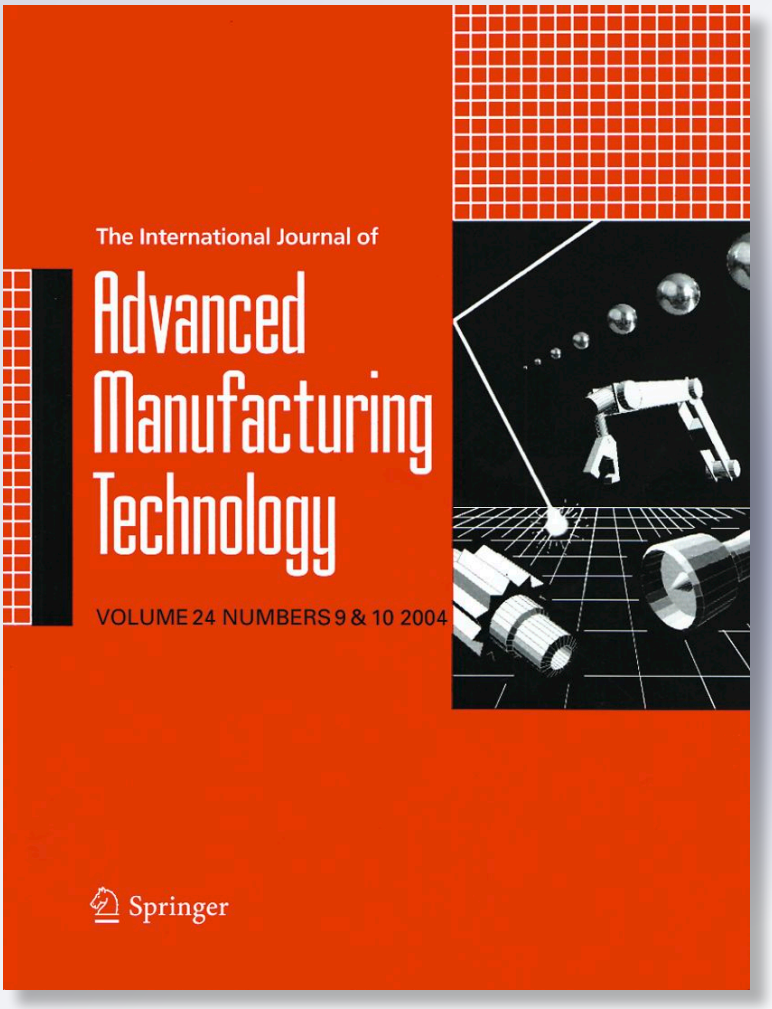

Springer

Int J Adv Manuf Technol (2012) 62:719–739
DOI 10.1007/s00170-011-3842-0

ORIGINAL ARTICLE

Interpolation of parametric CNC machining path under confined jounce

Wei Fan · Xiao-Shan Gao · Wei Yan · Chun-Ming Yuan

Received: 15 July 2011 / Accepted: 6 December 2011 / Published online: 3 January 2012

Abstract Aiming at reducing the computer numerically controlled (CNC) machining vibration and increasing machining quality, an interpolation method for parametric tool paths with confined jounce, jerk, acceleration, and speed is proposed. An acceleration/deceleration profile with confined jounce, jerk, acceleration, and speed is proposed, and it is shown that this profile is time optimal to change the speed from one value to another under the given constraints. For a given parametric tool path, the velocity function is obtained by first computing the critical points of the tool path where the radius of curvature reaches extremal values, then determining the feasible maximal speeds at the critical points, and finally using the jounce confined acceleration/deceleration profile to connect the speeds at the adjacent critical points. A vibration experiment is conducted, which shows that vibration of the CNC machine decreases significantly for motions under confined jounce than that under confined acceleration and jerk. Simulation for two real CNC models are given to show the feasibility of the method.

Keywords Interpolation · Velocity planning · Confined jounce · Time optimal · Parametric curve · Vibration · High-precision CNC machining

W. Fan · X.-S. Gao (✉) · W. Yan · C.-M. Yuan
KLMM, Academy of Mathematics and Systems Science, Chinese Academy of Sciences, Beijing 100190, China
e-mail: xgao@mmrc.iss.ac.cn
URL: http://www.mmrc.iss.ac.cn/~xgao/

1 Introduction

Interpolation algorithms, which control how the computer numerically controlled (CNC) machine tool moves along the machining path, is one of the important factors in high speed and high precision CNC machining. In particular, proper kinematic controls and interpolation algorithms are essential to reduce vibration and achieve high-precision CNC machining [12]. An interpolation algorithm in the CNC controller usually consists of two phases: velocity planning and parameter computation. Let $C(u)\, u \in [0, 1]$ be the machining path. The phase to determine the velocity function $v(u)$ along $C(u)$ is called velocity planning. When the velocity function $v(u)$ is known, the phase of sampling or computing the next interpolation point at parametric value $u_{i+1} = u_i + \triangle u$ during one sampling period is called parameter computation.

A key factor to compute the velocity function during velocity planning is to choose an acceleration/deceleration (AD) profile. An AD profile is the procedure to use different acceleration and deceleration modes to change the speed from one value to another under certain constraints.

The simplest AD profile is the linear AD profile, where the acceleration and speed are bounded or confined. Using a linear AD profile for each axis, Borow [2], Shiller et al. [13], and Farouki and Timar [14] presented a time-optimal velocity planning method for a parametric path. Zhang et al. simplified the method in [14] for quadratic B-splines and realized real-time machining on an industrial CNC machine [21]. Yuan, Zhang et al. presented a time-optimal velocity planning method with confined acceleration and chord error [18, 20].

In a linear AD profile, the acceleration can change instantaneously from its maximal value A to $-A$, resulting in large vibration of the CNC machine and decreasing the machining quality. A better AD profile is the *S-shape* profile, where the jerk is confined. The S-shape AD profile is widely used in velocity planning [3, 6, 8–11, 15, 19] to generate motion with confined jerk. Another method to obtain velocity functions with confined jerk is to use trigonometric function profiles [7]. Comparing to the S-shape profile, the acceleration function obtained with trigonometric function profiles is not differentiable. It also does not have the time-optimal property of the S-shape profile similar to Theorem 2.5 in this paper.

The S-shape AD profile increases the smoothness of the velocity function. However, the jerk can jump from its maximal value to its minimal value. Since change of the jerk reflects the non-smooth change of acceleration, the profile could still result in vibration and decrease machining quality. Gai et al. [5] used an average filter to improve the S-shape AD profile to obtain a continuous jerk in some extent. But this method fails to guarantee the continuity of acceleration and is not time optimal.

A natural way to obtain smoother velocity functions is to use confined jounce. Let F be the driving force of the CNC servo and F_c the combined cutting force and friction force. Denote the mass of the axes to be m and let j be jerk. Differentiate j to obtain

$$\frac{d^2(F-F_c)}{d^2t} = m\frac{dj}{dt} = ms, \tag{1}$$

where s is called the *jounce* or *snap*, which reflects the instantaneous change of jerk. If the jounce is confined, a motion with continuous jerk, differentiable acceleration, and C^2 velocity will be obtained. The main contribution of this paper is to design and investigate an AD profile with confined jounce and to present an interpolation algorithm for parametric tool paths based on the jounce confined AD profile.

The key component of the AD profile is a seven-period acceleration profile to increase the speed from one value to another. The whole AD profile first uses a seven-period acceleration profile to increase the speed from the initial value to its maximal value, then stays at the maximal value for a while, and finally uses a seven-period deceleration profile to decrease the speed from its maximal value to the end value. This paper analyzes the properties of the AD profile in detail and prove that this profile is time optimal to change the speed from one value to another under the given constraints.

For a curved tool path given by a set of parametric equations, the sensitive corner approach similar to that used in [7, 17] is used to compute its velocity function. Firstly, the critical points of the tool path, where the radius of curvature reaches extremal values, are computed. From these extremal values and a given sampling period, the maximal speeds that can be reached in these critical points are determined. Secondly, a backtracking procedure is used to check the reachability of the maximal speeds at each pair of neighboring critical points, that is, whether it is possible to change the maximal speed at one critical point to the maximal speed at the next critical point within the given tool path length. In the unreachable case, the speeds at the critical points are adjusted to make them reachable. Finally, between each pair of critical points, use the jounce confined AD profile to bridge their speeds, and the final velocity function is the combination of these AD profiles.

A vibration test experiment is carried out to compare AD profiles with confined acceleration, jerk, and jounce, which shows that the AD profile with confined jounce indeed can be used to reduce the vibration of the CNC machine tools and hence is useful to improve CNC machining quality. Furthermore, simulation results are given for two CNC models to show the feasibility of the proposed method.

The rest of this paper is organized as follows: In Section 2, the seven-period AD profile with confined jounce is designed and analyzed. In Section 3, the interpolation algorithm for parametric tool paths is proposed. In Section 4, experimental and simulation results are given. In Section 5, the paper is concluded.

2 An AD profile with confined jounce, jerk, acceleration, and speed

In this section, an AD profile for the speed to change from a start value v_s to an end value v_e within a distance d_m and under confined jounce will be presented. The profile is time optimal under the given conditions. Since the obtained velocity function has confined jounce, it is C^2 continuous.

2.1 A seven-period acceleration profile

In this section, a seven-period acceleration profile to increase the speed from zero to a given value $v_m > 0$ is introduced. The profile will serve as a basic step of our AD profile to be presented in Section 2.4.

The seven-period acceleration profile is given in Fig. 1, where the horizontal axis is time t. The profile is used to increase the speed from zero to $v_m > 0$ in seven periods as marked in the figure. If the speed is

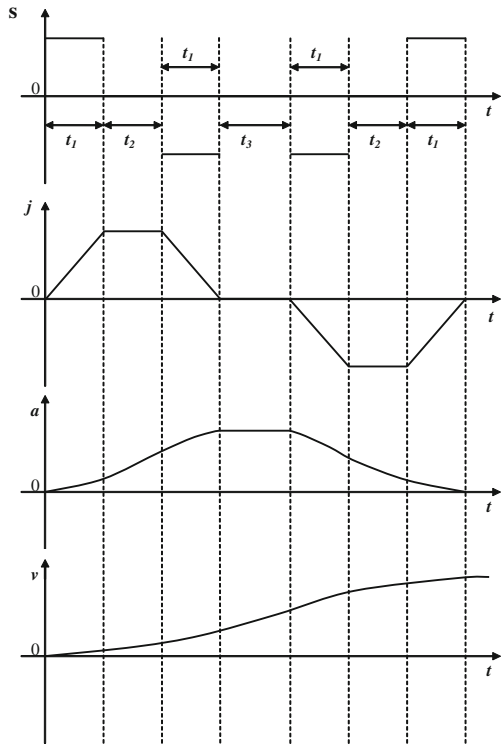

Fig. 1 Jounce (s), jerk (j), acceleration (a), and speed (v)

decreased from v_m to zero, then the reverse procedure can be used.

Make the basic assumption that the jounce is bounded by a given value S_m:

$$|s(t)| \le S_m. \tag{2}$$

At the start and end points, the acceleration and jerk are made to be zero, in order to form C^2 continuous velocity function with similar velocity profiles. That is

$$a_s = a_e = 0;\ j_s = j_e = 0.$$

As shown in Fig. 1, the first period with duration t_1 is used to increase the jerk from zero to its maximal value j_m with the maximal jounce S_m. In the second period with duration t_2, the jerk has constant value j_m and the acceleration is further increased. In the third period with duration t_1, the minimal jounce is used to decrease the jerk from j_m to zero and at the same time to increase the acceleration to its maximal value a_m. The fourth period with duration t_3 and with a constant acceleration a_m is used to further increase the speed. The last three periods are anti-symmetric with respect to the first three periods, which are used to increase the speed to its maximal value v_m and at the same time to decrease the acceleration from a_m to zero. The whole procedure lasts $t_m = 4t_1 + 2t_2 + t_3$. It is clear that the seven-period acceleration profile is "bang-bang" in the sense that at any time, at least one of the quantities $v(t), a(t), j(t), s(t)$ reaches its boundary value.

The seven-period profile is uniquely determined by the three parameters (t_1, t_2, t_3) and the maximal jounce S_m. Therefore, the triplet (t_1, t_2, t_3) is used to represent such a profile. After a triplet (t_1, t_2, t_3) is given, it is easy to obtain the expressions for $v_0(t), a(t), j(t), s(t), (t \in [0, t_m])$, which can be found in Eqs. 28 to 31 in the "Appendix" of this paper. It is clear that these expressions have the following form:

$$\begin{aligned} s(t) &= 6m_0 \\ j(t) &= 6m_0 t + 2m_1 \\ a(t) &= 3m_0 t^2 + 2m_1 t + m_2 \\ v_0(t) &= m_0 t^3 + m_1 t^2 + m_2 t + m_3 \end{aligned}$$

where m_i are constants depending on S_m; $s(t)$ is piecewise constant with three values 0, S_m, $-S_m$; $j(t)$ is piecewise linear; $a(t)$ is the integration of $j(t)$ about t and is C^1 piecewise linear or quadratic polynomials in t; and $v(t)$ is the integration of $a(t)$ about t and is C^2 continuous piecewise linear, quadratic, or cubic polynomials in t.

From Fig. 1 and the formulas 28 to 31, the maximal values j_m, a_m, v_m for $j(t), a(t), v_0(t)$ can be, respectively, obtained:

$$j_m = S_m t_1, \tag{3}$$

$$a_m = S_m(t_1 t_2 + t_1^2), \tag{4}$$

$$v_m = 2S_m t_1^3 + S_m t_1 t_2^2 + 3S_m t_1^2 t_2 + S_m t_1 t_2 t_3 + S_m t_1^2 t_3 \tag{5}$$

where S_m is from Eq. 2. As mentioned above, j_m is reached at $t = t_1$, a_m is reached at $t = 2t_1 + t_2$, and v_m is reached at $t = t_m = 4t_1 + 2t_2 + t_3$. The distance needed for the procedure can be computed as follows:

$$\begin{aligned} d_m &= 4S_m t_1^4 + 8S_m t_1^3 t_2 + S_m t_1 t_2^3 + 5S_m t_1^2 t_2^2 \\ &\quad + \frac{9}{2} S_m t_1^2 t_2 t_3 + \frac{3}{2} S_m t_1 t_2^2 t_3 \\ &\quad + \frac{1}{2} S_m t_1 t_2 t_3^2 + 3S_m t_1^3 t_3 + \frac{1}{2} S_m t_1^2 t_3^2 \\ &= \frac{v_m}{2}(4t_1 + 2t_2 + t_3). \end{aligned} \tag{6}$$

Now, suppose that the starting speed is v_s and the end speed is v_e. From Eq. 5,

$$v_e = v_s + 2S_m t_1^3 + S_m t_1 t_2 t_3 + S_m t_1 t_2^2 + 3S_m t_1^2 t_2 + S_m t_1^2 t_3. \tag{7}$$

Furthermore, it is easy to show that the distance of finishing the seven-period process is

$$\begin{aligned} d_{\min} &= 4S_m t_1^4 + 8S_m t_1^3 t_2 + S_m t_1 t_2^3 + 5S_m t_1^2 t_2^2 \\ &\quad + \frac{9}{2} S_m t_1^2 t_2 t_3 + \frac{3}{2} S_m t_1 t_2^2 t_3 + \frac{1}{2} S_m t_1 t_2 t_3^2 \\ &\quad + 3S_m t_1^3 t_3 + \frac{1}{2} S_m t_1^2 t_3^2 + v_s(4t_1 + 2t_2 + t_3) \qquad (8) \\ &= \frac{v_s + v_e}{2}(4t_1 + 2t_2 + t_3) = \frac{v_s + v_e}{2} t_m. \qquad (9) \end{aligned}$$

2.2 The acceleration profile for the speed to increase from v_s to v_e

This section will determine how to use the seven-period acceleration profile to increase the speed from v_s to v_e when the basic parameters of the CNC machine are given. It will be shown that the acceleration procedure is time optimal.

Three *basic parameters* of the CNC machine will be considered: the maximal jounce S_m, the maximal jerk J_m, and the maximal acceleration A_m. So, the constraints are

$$|a(t)| \le A_m, \; |j(t)| \le J_m, \; |s(t)| \le S_m. \qquad (10)$$

Since the seven-period acceleration profile is used, the initial conditions are

$$a_s = a(0) = a_e = a(t_m) = 0; \quad j_s = j(0) = j_e = j(t_m) = 0. \qquad (11)$$

Without loss of generality, assume that $v_s \le v_e$.

The purpose of this section is to determine a seven-period acceleration profile to increase the speed from v_s to v_e under the constraints 10 and 11. The distance needed for the acceleration procedure is also given. But the constraint on the distance is not considered in this section. As mentioned before, to determine the seven-period acceleration profile, one just needs to determine (t_1, t_2, t_3).

Firstly, check whether $t_2 = 0$ based on the values of S_m, J_m, A_m. From Eqs. 3 and 4,

$$S_m a_m = S_m j_m t_2 + j_m^2. \qquad (12)$$

Three cases are considered. If ${J_m}^2 > S_m A_m$, then the jerk cannot reach J_m and t_2 must be zero. Assume the contrary, from Eq. 12, $J_m^2 + S_m t_2 J_m = S_m a_m$. Since $0 \le a_m \le A_m$, $t_2 = (S_m a_m - J_m^2)/(S_m J_m)$ must be negative, which is impossible. As a consequence, $t_2 = 0$.

If ${J_m}^2 = S_m A_m$, j reaches J_m at $t_1 = J_m/S_m$ and $t_2 = 0$. When $t = 2t_1$, the acceleration reaches A_m.

If ${J_m}^2 < S_m A_m$ and under the assumption that there exist no constraints on the final speed and the distance, then from Eqs. 3 and 12, the jerk reaches J_m at $t_1 = J_m/S_m$, the acceleration reaches A_m at $t = 2t_1 + t_2$, and $t_2 = (S_m A_m - J_m^2)/(S_m J_m) > 0$. Of course, if there exist constraints on the final speed v_m, then t_2 might be zero, which will be discussed later.

Summarize the above analysis as the following proposition:

Proposition 2.1

1. *If ${J_m}^2 \ge S_m A_m$, then $t_2 = 0$. In this case, the jerk j cannot reach the maximal value J_m unless the equal sign holds.*
2. *If ${J_m}^2 < S_m A_m$ and there exist no other constraints, then the jerk reaches J_m at $t_1 = J_m/S_m$, the acceleration reaches A_m at $t = 2t_1 + t_2$, and $t_2 = (S_m A_m - J_m^2)/(S_m J_m) > 0$.*

In the above analysis, the constraint raised from the final speed v_m is not considered. Now consider how to increase the speed from zero to v_m with the seven-period acceleration profile by taking into account of v_m. Two cases are considered due to Proposition 2.1.

Case 1. ${J_m}^2 \ge S_m A_m$. By Proposition 2.1, $t_2 = 0$. If the acceleration reaches A_m, then from Eq. 4 $t_1 = \sqrt{A_m/S_m}$. Let

$$v_0 = 2S_m t_1^3 = 2S_m \left(\frac{A_m}{S_m}\right)^{\frac{3}{2}}.$$

Then (t_1, t_2, t_3) can be determined as follows:

Case 1.1 If $v_m > v_0$, then $a(t)$ reaches A_m at $t = 2t_1 = 2\sqrt{\frac{A_m}{S_m}}$. In order to reach v_m, there exists a constant acceleration phase t_3 which can be computed from Eq. 5 as follows:

$$\begin{aligned} t_3 &= \frac{v_m - 2S_m t_1^3}{S_m t_1^2} = \frac{v_m - 2S_m t_1^3}{A_m} \\ &= \frac{v_m - v_0}{A_m} > 0, \qquad (13) \end{aligned}$$

where $t_1 = \sqrt{\frac{A_m}{S_m}}$.

For $i = 1, 2, 3$, introduce the symbol $\widehat{t_i} = +$ if $t_i \ne 0$ and $\widehat{t_i} = -$ if $t_i = 0$. Then use $(\widehat{t_1}, \widehat{t_2}, \widehat{t_3})$ to denote the shape of the seven-period acceleration profile. In case 1.1, the acceleration profile is $(+, -, +)$ which is shown in Fig. 2c.

Case 1.2 If $v_m \le 2S_m(\frac{A_m}{S_m})^{\frac{3}{2}}$, then the acceleration will not reach A_m unless the equality holds. Assume the contrary, from Eq. 13, t_3 will be negative, which is impossible. Therefore, $t_3 = 0$ and t_1 will be determined by v_m with formula 5: $t_1 = \sqrt[3]{\frac{v_m}{2S_m}}$. Then, the acceleration profile is $(+, -, -,)$ which is shown in Fig. 2d.

Case 2. ${J_m}^2 < S_m A_m$. By Proposition 2.1, if the jerk reaches J_m, then $t_1 = J_m/S_m$, and if the acceleration reaches A_m, then $t_2 = (S_m A_m - J_m^2)/(S_m J_m)$. Under the above-mentioned conditions, set

$$v_1 = 2S_m t_1^3 = \frac{2J_m^3}{S_m^2}.$$

$$v_2 = 2S_m t_1^3 + S_m t_1 t_2^2 + 3S_m t_1^2 t_2 = \frac{A_m(S_m A_m + J_m^2)}{S_m J_m}.$$

Then (t_1, t_2, t_3) can be determined as follows:

Case 2.1 If $v_m > v_2$, then both the jerk and the acceleration reach their maximal values and $t_3 \ne 0$ can be computed from Eq. 5 as follows:

$$t_3 = \frac{v_m - v_2}{A_m} = \frac{v_m}{A_m} - \left(\frac{J_m}{S_m} + \frac{A_m}{J_m}\right).$$

The acceleration profile is $(+, +, +)$ which is shown in Fig. 2a.

Case 2.2 If $v_1 < v_m \le v_2$, then $t_3 = 0$, the jerk can reach J_m, and $a(t)$ cannot reach A_m unless $v_m = v_2$. Furthermore, t_2 is determined by v_m from Eq. 5 with the following formula:

$$t_2 = \frac{\sqrt{t_1^2 + \frac{4v_m}{J_m}} - 3t_1}{2} = \frac{\sqrt{J_m^3 + 4v_m S_m^2} - 3J_m^{\frac{3}{2}}}{2S_m\sqrt{J_m}}$$

The acceleration profile is $(+, +, -)$ which is shown in Fig. 2b.

Case 2.3 If $v_m \le v_1$, then neither the jerk (unless $v_m = v_1$) nor the acceleration reaches their maximal values and $t_2 = t_3 = 0$. Furthermore, t_1 is determined by v_m from Eq. 5 as follows:

$$t_1 = \sqrt[3]{\frac{v_m}{2S_m}}.$$

The acceleration profile is $(+, -, -)$ which is shown in Fig. 2d.

Based on the above analysis, the algorithm to increase the speed from v_s to v_e with the seven-period

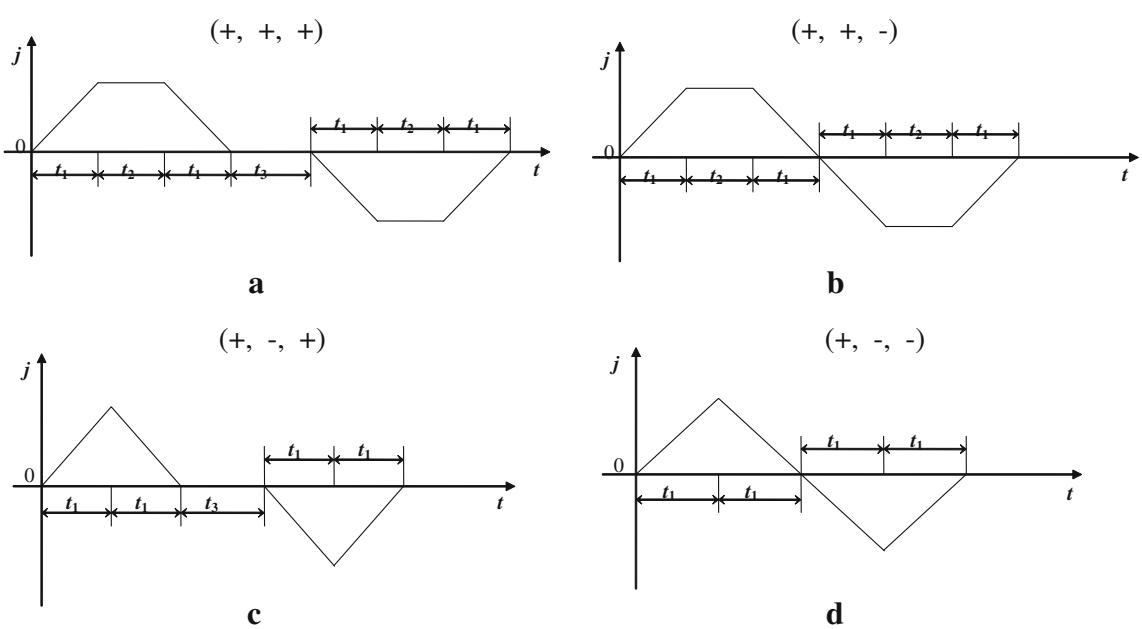

Fig. 2 **a–d** Jerk functions for all possible acceleration profiles

Algorithm 2.2 PRO_VV(v_s,v_e)

Input: Parameters S_m, J_m, A_m in Eq. 10, the start speed v_s and end speed v_e.
Output: The parameters (t_1, t_2, t_3) of the seven-period acceleration profile.

1. Let $v^* = |v_e - v_s|$. If ${J_m}^2 \geq S_m A_m$, then go to step 2; else go to step 3.
2. Compute t_1, t_2, t_3 by the following formulas and output (t_1, t_2, t_3).

$$\begin{cases} t_1 = \sqrt{\dfrac{A_m}{S_m}}, t_2 = 0, t_3 = \dfrac{v^* - 2S_m t_1^3}{A_m}, & \text{if } v^* > 2S_m(\dfrac{A_m}{S_m})^{\frac{3}{2}}, \\ t_1 = \sqrt[3]{\dfrac{v^*}{2S_m}}, t_2 = 0, t_3 = 0, & \text{if } v^* \leq 2S_m(\dfrac{A_m}{S_m})^{\frac{3}{2}} \end{cases}$$

3. Compute t_1, t_2, t_3 by the following formulas and output (t_1, t_2, t_3):

$$\begin{cases} t_1 = \dfrac{J_m}{S_m}, t_2 = \dfrac{A_m - \frac{J_m^2}{S_m}}{J_m}, t_3 = \dfrac{v^* - (2S_m t_1^3 + 3S_m t_1^2 t_2 + S_m t_1 t_2^2)}{A_m}, & \text{if } v^* > \dfrac{A_m^2}{J_m} + \dfrac{A_m J_m}{S_m}, \\ t_1 = \dfrac{J_m}{S_m}, t_2 = \dfrac{\sqrt{t_1^2 + \dfrac{4v^*}{J_m}} - 3t_1}{2}, t_3 = 0, & \text{if } \dfrac{2J_m^3}{S_m^2} < v^* \leq \dfrac{A_m^2}{J_m} + \dfrac{A_m J_m}{S_m}, \\ t_1 = \sqrt[3]{\dfrac{v^*}{2S_m}}, t_2 = 0, t_3 = 0, & \text{if } v^* \leq \dfrac{2J_m^3}{S_m^2} \end{cases}$$

acceleration profile can be given. If $v_s > v_e$, a decrease profile can be designed similarly. Also assume that the distance is long enough for the procedure to carry out. The constraints on the distance will be considered in Section 2.4.

Using the notation $(\widehat{t_1}, \widehat{t_2}, \widehat{t_3})$, Algorithm **PRO_VV** can be summarized as the flowchart in Fig. 3.

It is clear that the selections of the parameters t_1, t_2, t_3 are not unique. For instance, in case 1, we can increase the jerk to a value $j_m < J_m$ and then include a constant jerk part $t_2 > 0$. Also, in case 2, if mode $(+,+,+)$ fails, it seems that both $(+,+,-)$ and $(+,-,+)$ can be chosen. The following theorem will show that our choosing method for the parameters leads to a time-optimal solution to the problem. The proof of the theorem can be found in "Appendix" of this paper.

Theorem 2.3 *Algorithm* **PRO_VV** *is a time-optimal procedure to increase the speed from* v_s *to* v_e *under the constraints* 10 *and* 11.

2.3 The acceleration profile with initial speed v_s and distance d_m

In this section, an acceleration profile will be given to compute the maximal speed that can be reached with a start speed v_s and a given distance d_m.

Similar to Section 2.2, we need to compute the parameters (t_1, t_2, t_3) for the seven-period acceleration profile by considering two cases.

Case 1. ${J_m}^2 \geq S_m A_m$. By Proposition 2.1, $t_2 = 0$. If the acceleration reaches A_m, then from Eq. 4 $t_1 = \sqrt{A_m/S_m}$. Let

$$d_0 = 4S_m t_1^4 + 4v_s t_1 = 4\frac{A_m^2}{S_m} + 4v_s\sqrt{\frac{A_m}{S_m}}. \quad (14)$$

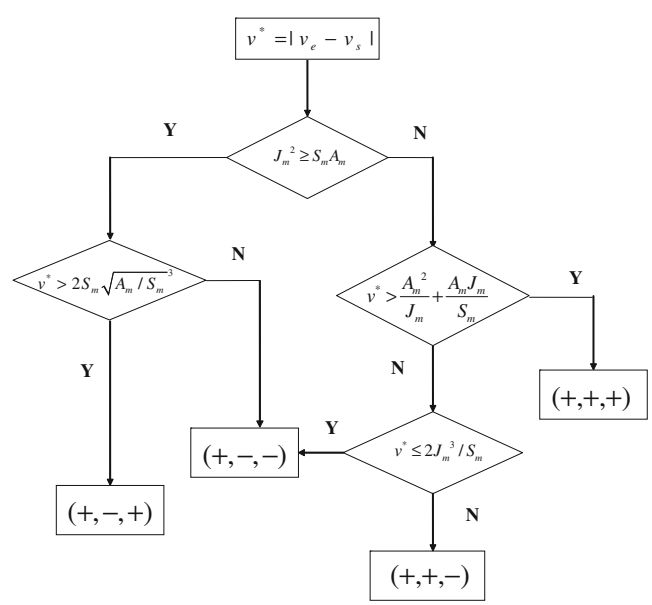

Fig. 3 Flowchart for Algorithm **PRO_VV**

Then (t_1, t_2, t_3) can be determined as follows:

Case 1.1 If $d_m > d_0$, then A_m is reachable and $t_1 = \sqrt{A_m/S_m}$. Furthermore, there exists a constant acceleration period $t_3 \neq 0$. From Eq. 9, t_3 can be computed by solving the following quadratic equation in t_3:

$$d_m = 4S_m t_1^4 + 3S_m t_1^3 t_3 + \frac{1}{2} S_m t_1^2 t_3^2 + v_s(4t_1 + t_3). \quad (15)$$

It is easy to show that the above equation has a unique positive solution due to the fact $d_m > d_0$. The acceleration profile is $(+, -, +)$ which is shown in Fig. 2c.

Case 1.2 If $d_m \leq d_0$, then A_m is not reachable (unless $d_m = d_0$) and $t_3 = 0$. Furthermore, t_1 is determined by d_m based on Eq. 9 by solving the following equation in t_1:

$$d_m = 4S_m t_1^4 + 4v_s t_1. \quad (16)$$

The acceleration profile is $(+, -, -)$ which is shown in Fig. 2d.

Case 2. ${J_m}^2 < S_m A_m$. By Proposition 2.1, if the jerk reaches J_m, then $t_1 = J_m/S_m$, and if the acceleration reaches A_m, then $t_2 = (S_m A_m - J_m^2)/(S_m J_m)$. Under the above-mentioned conditions, set

$$\begin{aligned} d_1 &= 4S_m t_1^4 + 4v_s t_1 = 4\frac{J_m^4}{S_m^3} + 4v_s \frac{J_m}{S_m} \\ d_2 &= 4S_m t_1^4 + 8S_m t_1^3 t_2 + S_m t_1 t_2^3 \\ &\quad + 5S_m t_1^2 t_2^2 + v_s(4t_1 + 2t_2) \\ &= A_m\left(\frac{A_m}{J_m} + \frac{J_m}{S_m}\right)^2 + 2v_s\left(\frac{A_m}{J_m} + \frac{J_m}{S_m}\right). \end{aligned} \quad (17)$$

Then (t_1, t_2, t_3) can be determined as follows:

Case 2.1 If $d_m > d_2$, then both the jerk and acceleration can reach their maximal values and the constant acceleration phase $t_3 \neq 0$ which can be computed by solving the quadratic equation 9 in t_3. The acceleration profile is $(+, +, +)$ which is shown in Fig. 2a.

Case 2.2 If $d_1 < d_m \leq d_2$, then the jerk can reach J_m and the acceleration cannot reach A_m unless $d_m = d_2$. Therefore, the stage of constant acceleration $t_3 = 0$ and t_2 is determined from Eq. 9 with d_m by solving the quadratic equation in t_2

$$d_m = 4S_m t_1^4 + 8S_m t_1^3 t_2 + S_m t_1 t_2^3 + 5S_m t_1^2 t_2^2 + +v_s(4t_1 + 2t_2).$$

The acceleration profile is $(+, +, -)$ which is shown in Fig. 2b.

Case 2.3 If $d_m \leq d_1$, then neither the jerk (unless $d_m = d_1$) nor the acceleration reaches their maximal value and $t_2 = t_3 = 0$. Further, t_1 is determined from Eq. 9 with d_m by solving the equation: $d_m = 4S_m t_1^4 + 4v_s t_1$. The acceleration profile is $(+, -, -)$ which is shown in Fig. 2d.

Algorithm 2.4 PRO_VD(v_s,d_m)

Input: Parameters S_m, J_m, A_m in Eq. 10, the start speed v_s, and a distance d_m.

Output: The parameters (t_1, t_2, t_3) of the seven-period acceleration profile.

1. If ${J_m}^2 \geq S_m A_m$, then go to step 2; else go to step 3.
2. Let $t_2 = 0$ and d_0 be given by Eq. 14. If $d_m > d_0$, set $t_1 = \sqrt{A_m/S_m}$ and compute t_3 with Eq. 15; otherwise, set $t_3 = 0$ and compute t_1 with Eq. 16. Output (t_1, t_2, t_3).
3. Let d_1 and d_2 be given in Eq. 17.

$$\begin{cases} t_1 = \dfrac{J_m}{S_m}, t_2 = \dfrac{A_m - \frac{J_m^2}{S_m}}{J_m}, \\ \quad \text{solve Eq. 9 to find } t_3, & \text{if } d_m > d_2 \\ t_1 = \dfrac{J_m}{S_m}, t_3 = 0, \\ \quad \text{solve Eq. 9 to find } t_2, & \text{if } d_1 < d_m \leq d_2 \\ t_2 = t_3 = 0, \text{ solve Eq. 9 to find } t_1, & \text{if } d_m \leq d_1 \end{cases}$$

Output (t_1, t_2, t_3).

Based on the above analysis, we give the algorithm to determine the end speed with a start speed v_s and a distance d_m. Again, the output of the algorithm is the parameters (t_1, t_2, t_3), with which the end speed v_e can be computed with Eq. 7 and the speed function $v(t)$ can

be computed as $v(t) = v_s + v_0(t)$ where $v_0(t)$ is defined in Eq. 31.

Similar to Theorem 2.3, it can be shown that the algorithm is optimal in that it can give the maximal end speed when using the seven-period acceleration profile.

Theorem 2.5 *Algorithm* **PRO_VD** *outputs the maximal speed that can be reached with the start speed v_s and the distance d_m with the seven-period acceleration profile.*

Algorithm **PRO_VD**(v_s,d_m) can be modified easily to compute the minimal speed that can be reached from v_s within distance d_m.

2.4 The AD profile with confined jounce, jerk, acceleration, and speed

With the preparations given in Sections 2.2 and 2.3, now a complete AD profile can be given to change the speed from v_s to v_e with distance d_m and under the given jounce, jerk, acceleration, and speed bounds. As shown in Fig. 4, the AD profile consists of three phases composed by 15 periods. Firstly, the speed is increased from the start speed v_s to the maximal speed V_m with a seven-period acceleration profile; secondly, the speed keeps the constant value V_m; and thirdly, the speed decreases from V_m to the end speed v_e with a seven-period deceleration profile. Let (t_1, t_2, t_3) be the parameters for the seven-period acceleration profile in the first phase, t_4 the time for the constant speed phase, and (t_5, t_6, t_7) the parameters for the seven-period deceleration profile in the third phase. Then the AD profile can be uniquely determined by the seven parameters $(t_1, t_2, t_3, t_4, t_5, t_6, t_7)$ and its velocity function can be computed with formula 18. Due to the initial conditions 11 of the seven-period profile, the velocity function of the AD profile is C^2 continuous.

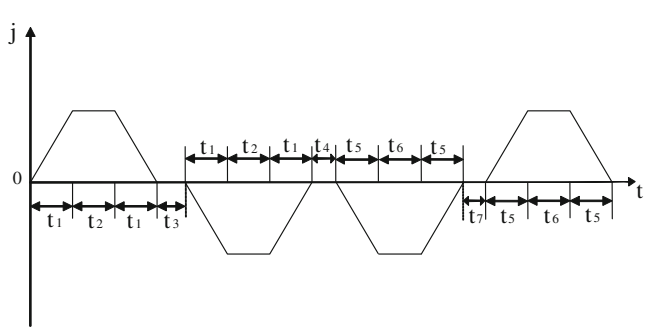

Fig. 4 Jerk function for 15-period AD profile

$$\bar{v}(t) = \begin{cases} v_s + v_0(t),\ v_0(t) \text{ is from} & \\ \quad \text{Eq. 31 with } (t_1, t_2, t_3), & t \in [0, t_{m_1}] \\ V_m, & t \in [t_{m_1}, t_{m_1} + t_4] \\ V_m - v_0(t - t_{m_1} - t_4),\ v_0(t) & \\ \quad \text{is from Eq. 31} & \\ \quad \text{with } (t_5, t_6, t_7), & t \in [t_{m_1} + t_4, t_m] \end{cases} \tag{18}$$

where $t_{m_1} = 4t_1 + 2t_2 + t_3$, $t_{m_2} = 4t_5 + 2t_6 + t_7$, $t_m = t_{m_1} + t_4 + t_{m_2}$. From Eq. 9, the distance for the AD profile is

$$d = \frac{(v_s + V_m)t_{m_1}}{2} + t_4 V_m + \frac{(v_e + V_m)t_{m_2}}{2}. \tag{19}$$

First, a brief introduction to the algorithm is given. Without loss of generality, assume $v_s \le v_e$. Firstly, check the reachability of v_e from v_s within distance d_m. The minimal distance d_{min} for accelerating from v_s to v_e can be determined using Algorithm **PRO_VV**(v_s, v_e). If $d_m \ge d_{min}$, then v_e is reachable; otherwise, the algorithm terminates.

Now suppose v_e is reachable. Algorithms **PRO_VV** (v_s, V_m) and **PRO_VV**(v_e, V_m) can be used to compute the minimal distances d_i and d_d for the speed to increase from v_s to V_m and to decrease from V_m to v_e. If $d_i + d_d \le d_m$, then V_m is reachable and there is a phase of constant speed V_m.

If $d_i + d_d > d_m$, then V_m is not reachable and one needs to compute the practical reachable maximal speed v_m. The speed v_m can be computed by solving a set of algebraic equations. But due to the complicated selection procedure for the parameters $t_i, i = 1, 2, 3, 5, 6, 7$, this approach is not practical. Instead, an iteration procedure will be used to compute v_m. Set $v_0 = V_m$, $v_1 = v_e$, and $v_2 = (v_0 + v_1)/2$. Then compute the distances d_i and d_d for the speed to increase from v_s to v_2 and to decrease from v_2 to v_e. If $d_i + d_d \le d_m$, then v_2 is reachable and set $v_0 = \max\{v_0, v_1\}$, $v_1 = v_2$. Otherwise, v_2 is unreachable and set $v_1 = \min\{v_0, v_1\}$, $v_0 = v_2$. Repeat the above bisection procedure until $|d_{i0} + d_{d0} - d_m|$ is smaller than a given precision and use the last computed value of v_2 as v_m.

With the above analysis, the algorithm to find the AD profile is given below.

Based on Theorems 2.3 and 2.5, it can be shown that the above algorithm is time optimal.

Theorem 2.6 *Algorithm* **PRO_AD** *outputs a time-optimal procedure for the speed to change from v_s to v_e with distance d_m under the constraints 10 and 11.*

Algorithm 2.5 PRO_AD(v_s, v_e, d_m)

Input: Parameters S_m, J_m, A_m, V_m, the start speed v_s, the end speed v_e, and the distance d_m.

Output: The speed v_e is unreachable, or the parameters $(t_1, t_2, t_3, t_4, t_5, t_6, t_7)$ for the AD profile.

1. Compute (t_1, t_2, t_3) with Algorithm **PRO_VV**(v_s, v_e). Set d_{min} to be the distance computed with formula 9 and (t_1, t_2, t_3). If $d_{min} > d_m$, then v_e is unreachable and the algorithm terminates.
2. Let (t_1, t_2, t_3) and (t_5, t_6, t_7) be the outputs of Algorithm **PRO_VV**(v_s, V_m) and Algorithm **PRO_VV** (v_e, V_m), respectively, and d_i and d_d the distances for the speed to increase from v_s to V_m and to decrease from V_m to v_e computed with formula 9.
3. If $d_i + d_d \leq d_m$, then V_m is reachable. Compute $t_4 = (d_m - d_i - d_d)/V_m$. Outputs $(t_1, t_2, t_3, t_4, t_5, t_6, t_7)$.
4. Now $d_i + d_d > d_m$ and V_m is unreachable. Set $t_4 = 0$, $v_0 = V_m$, $v_1 = v_e$, $\epsilon = 10^{-4}$.
   a. Set $v_2 = (v_0 + v_1)/2$.
   b. Let (t_1, t_2, t_3) and (t_5, t_6, t_7) be the outputs of Algorithms **PRO_VV**(v_s, v_2) and **PRO_VV** (v_e, v_2), respectively, and d_i and d_d the distances for the speed to increase from v_s to v_2 and to decrease from v_2 to v_e computed with formula 9.
   c. If $|d_i + d_d - d_m| < \epsilon$, outputs $(t_1, t_2, t_3, t_4, t_5, t_6, t_7)$.
   d. If $d_i + d_d \leq d_m$, then v_2 is reachable. Let $v_0 = \max\{v_0, v_1\}$, $v_1 = v_2$. Go to step (a).
   e. Now $d_i + d_d > d_m$ and v_2 is unreachable. Let $v_1 = \min\{v_0, v_1\}$, $v_0 = v_2$. Go to step (a).

3 Interpolation of parametric tool path with confined jounce

In this section, an interpolation method along a parametric tool path with confined jounce, jerk, acceleration, and speed will be proposed.

The algorithm works as follows: Firstly, by a transversal of the tool path, the critical points of the too path, where the radius of curvature reaches local extremal values, are obtained. Due to the relation between the chord error and speed, the maximal machining speed also reaches local extremal values at these points, which are called limit speeds. Secondly, by a backtracking algorithm, the limit speeds of the critical points are adjusted to make them reachable. Finally, Algorithm **PRO_VV** or Algorithm **PRO_AD** is used to interpolate a segment of the tool path between two adjacent critical points.

3.1 Critical points on the tool path

This section will show how to compute the points on the tool path where the limit machining speed reaches local extremal values. Let the tool path be a kth-order B-spline curve with expression

$$C(u) = \{x(u), y(u), z(u)\} = \sum_{i=0}^{n} Q_i N_{i,k}(u), \quad 0 \leqslant u \leqslant 1 \tag{20}$$

where Q_i $(i = 0, 1, \ldots, n)$ are the $n+1$ control points, $N_{i,k}(u)$ are the basis functions of kth-order B-splines based on the knot vector $\mathbf{T} = \{t_0, t_1, \ldots, t_{n+k+1}\}$, and u is the parameter. Note that other parametric curves such as NURBS can be treated similarly.

Denote *the parametric speed* of $C(u)$ to be

$$\sigma(u) = \frac{ds}{du} = |C'(u)|,$$

where $'$ is the derivative w.r.t. u. The *curvature* and *radius of curvature* are defined to be

$$\kappa(u) = \frac{|C'(u) \times C''(u)|}{\sigma(u)^3}, \rho(u) = \frac{1}{k(u)}. \tag{21}$$

It is well-known that at a point $u = u_0$ of the tool path $C(u)$, the interpolation speed is limited by the given chord error δ. Expanding $C(u)$ in the neighborhood of $C(u_0)$ with the following Taylor formula:

$$C(u_0 + \Delta u) = C(u_0) + \mathbf{a}_0 \Delta u + \frac{1}{2}\kappa_0 \mathbf{b}_0 (\Delta u)^2 + \frac{1}{6}(-\kappa_0^2 \mathbf{a}_0 + \dot{\kappa}_0 \mathbf{b}_0 + \kappa_0 \tau_0 \mathbf{c}_0 + \epsilon)(\Delta u)^3, \tag{22}$$

where κ_0, τ_0 are the curvature and torsion, respectively, $\mathbf{a}_0$, $\mathbf{b}_0$, $\mathbf{c}_0$ are the values of tangential vector $\mathbf{a}$, the principal normal vector $\mathbf{b}$, the binormal vector $\mathbf{c}$ at $u = u_0$, and ϵ is a tiny quantity.

According to Eq. 22, when using line segments to approximate the spline curve, the second-order residual term is only related with the curvature and the third-order term is related with the torsion. Therefore, a circle whose radius is $\rho(u_0)$ can approximate the curve locally. The contour error of the interpolation is limited by the chord error δ which is caused by approximating the real curve using the short line segment within one sampling period.

Let δ be the chord error bound and Δu the maximal possible increase of the parameter u without violating the chord error bound. Thus, the following well-known relationship is obtained [18]:

$$\Delta L(u) = |C(u)C(u + \Delta u)| \approx \sqrt{8\rho\delta}.$$

Let T be the sampling period. So the maximal possible speed at point $C(u)$ constrained by the chord error bound is

$$v_{\lim}(u) = \Delta L(u)/T = \sqrt{8\rho(u)\delta}/T. \tag{23}$$

The speed $v_{\lim}(u)$ is called the *limit speed* at point $C(u)$.

According to Eq. 23, $v_{\lim}(u)$ has the same extremal points with the radius of curvature function $\rho(u)$, which has the same extremal points with the curvature function $\kappa(u)$ by Eq. 21. These extremal points are called *critical points* of the tool path. The extremal points of $v_{\lim}(u)$ can be computed by solving the following algebraic equations in u for each piece of the curve $C(u)$.

$$\kappa(u)' = 0. \tag{24}$$

Furthermore, if the continuity of the spline at the connection point is less than C^2, then these points need to be treated as critical points and the minimal value of the limit speeds of the two curve segments at the connect point is taken as the limit speed.

The extremal points can also be computed in a discrete way as follows: First make a traversal of the curve $C(u), u \in [0, 1]$ with the speed $v_{\lim}(u)$ and a given sampling period T to find interpolation points $u_0 = 0, u_1, \ldots, u_n = 1$. Then we may find the extremal points from the values $v_{\lim}(u_i)$. Based on the above analysis, the following algorithm is given to compute the extremal points.

Algorithm 3.1 CR_PTS($C(u), u \in [0, 1]$)

Input: B-spline curve $C(u), u \in [0, 1]$, the sampling period T, the maximal speed V_{m} of the CNC machining.
Output: Parametric values of the critical points $u_i, i = 0, \ldots, N$.

1. Use Algorithm 3.5 with inputs $C(u), u \in [0, 1]$ and $v_{\lim}(u), u \in [0, 1]$ (step size at $u = u_0$ can be found as $\Delta L = \min(v_{\lim}(u_0), V_{\mathrm{m}})T$) to find the interpolation points $\bar{u}_0 = 0, \bar{u}_1, \ldots, \bar{u}_{\mathrm{m}} = 1$.
2. Select the parameters $\bar{u}_k$ correspond to the extremal points. That is, the $\bar{u}_k$ satisfying

   $$(v_{\lim}(\bar{u}_k) - v_{\lim}(\bar{u}_{k-1}))(v_{\lim}(\bar{u}_k) - v_{\lim}(\bar{u}_{k+1})) \geq 0.$$

   Denote these parameters as $u_1, \ldots, u_{N-1}$. Output $u_0 = 0, u_1, \ldots, u_{N-1}, u_N = 1$.

Remark 3.2 When the parametric curve is simple, the extremal points can be found by directly solving Eq. 24. For parametric curves with high degrees, use Algorithm 3.1 to compute the extremal points.

Let $C(u_i), i = 0, \ldots, N$ be the points found with the above algorithm. If the limit speed $v_{\lim}(u)$ achieves a local minimal (maximal) value at u_i, then u_i is called a *minimal (maximal) critical point*. If the curve $C(u)$ is at least second-order differentiable, minimal and maximal critical points occur alternatively.

3.2 Reachability test

The limit speeds at the critical points might not be reachable due to the constraints of distance between two adjacent critical points. It is necessary to check reachability of the speeds at two adjacent critical points and adjust the unreachable speeds to make them reachable.

Consider the reachability from point $C(u_k)$ with limit speed v_k to $C(u_{k+1})$ with limit speed $\hat{v}_{k+1}$. Let L_k be the length of the curve segment $C(u), u \in [u_k, u_{k+1}]$. With Algorithm **PRO_VD**(v_k, L_k), compute the maximal speed v^+ that can be reached from v_k within distance L_k and the minimal speed v^- that can be reached from v_k within distance L_k. If $v^- \leq \hat{v}_{k+1} \leq v^+$, then $v_{k+1} = \hat{v}_{k+1}$ is reachable. If $\hat{v}_{k+1} > v^+$, then v_k cannot increase to $\hat{v}_{k+1}$ and set $v_{k+1} = v^+$. If $v^- > \hat{v}_{k+1}$, then v_k cannot decrease to $v_{k+1} = \hat{v}_{k+1}$, and it is necessary to do a backtracking by checking the reachability starting from point u_{k+1} in the backward direction.

Based on the above analysis, the reachability test and adjustment algorithm is given below.

Let $C(u_i), i = 0, \ldots, N$ be the *critical points*. After the adjustments, the speeds at certain critical points are decreased and the property of alternating minimal and maximal speeds is not true anymore. So delete some of the critical points to make the speed alternatively minimal and maximal again. That is, a point u_i is removed if $(v_i - v_{i-1})(v_i - v_{i+1}) < 0$. Note that this strategy enhances the interpolation speed.

3.3 Interpolation with confined jounce

In this section, an algorithm will be given to achieve interpolation with confined jounce, jerk, acceleration, and speed. And the chord error is kept as small as possible. As usual, the interpolation procedure is divided into two phases: the velocity planning phase to find the velocity function and the parameter computing phase to find the interpolation points.

Algorithm 3.3 REACH($u_i, i = 0, \ldots, N$)

Input: Critical points $u_i, i = 0, \ldots, N$ of the tool path $C(u)$ assuming $u_0 = 0$ and $u_N = 1$. The sampling period T and the maximal speed V_m of the CNC machining.
Output: Reachable speeds $v_k, i = 0, \ldots, N$ at the critical points.

1. Set $i = 0$, $v_0 = 0$, $v_N = 0$.
2. If $i = N$, then terminate the algorithm; otherwise, let L_i be the length of the curve segment $C(u), u \in [u_i, u_{i+1}]$.
3. Using Algorithm **PRO_VD**(v_i, L_i) to compute the maximal speed v^+ and minimal speed v^- that can be reached from v_i with distance L_i.
4. If $i + 1 = N$, then set $\hat{v}_{i+1} = 0$; else set $\hat{v}_{i+1} = \min\{v_\mathrm{lim}(u_{i+1}), V_\mathrm{m}\}$, where v_lim is defined in Eq. 23.
5. If $v^- \le \hat{v}_{i+1} \le v^+$, then $\hat{v}_{i+1}$ is reachable, set $v_{i+1} = \hat{v}_{i+1}, i = i + 1$, go to step 2.
6. If $\hat{v}_{i+1} > v^+$, then set $v_{i+1} = v^+, i = i + 1$, go to step 2.
7. If $\hat{v}_{i+1} < v^-$, then set $v_{i+1} = \hat{v}_{i+1}, i = i + 1, j = i$ and execute the following backtracking steps.
   (a) Using Algorithm **PRO_VD**(v_j, L_{j-1}) to compute the maximal speed v^* that can be reached from v_j with distance L_{j-1}.
   (b) If $v_{j-1} \le v^*$, then from v_{j-1} to v_j is reachable. Go to step 2.
   (c) If $v_{j-1} > v^*$, then from v_{j-1} to v_j is not reachable. Set $v_{j-1} = v^*$, $j = j - 1$, and if $j \ge 2$, then go to step (a); else go to step 2.

First, consider the velocity planning phase. Let $C(u_i), i = 0, \ldots, N$ be the critical points of the tool path $C(u)$. Then, from point $C(u_i)$ to $C(u_{i+1})$, the limit speed is either monotonously increasing or monotonously decreasing. As a consequence, Algorithm **PRO_VV** can be used to interpolate the tool path segments between two adjacent critical points.

Let $v(t), t \in [0, t_\mathrm{m}]$ be the speed function obtained with Algorithm **PRO_VV**(v_i, v_{i+1}), d_m computed with Eq. 9, and L_i the length of the curve segment $C(u), u \in [u_i, u_{i+1}]$. Then $\bar{v}(t) = v(\frac{t d_\mathrm{m}}{L_i}), t \in [0, \frac{t_\mathrm{m} L_i}{d_\mathrm{m}}]$ is a speed function which increases the speed from v_i to v_{i+1}. Since the distance for this procedure is L_i, $\bar{v}(t)$ interpolates the curve segment $C(u), u \in [u_i, u_{i+1}]$. Note that between two adjacent critical points, $\bar{v}(t)$ and the velocity limit curve $v_\mathrm{lim}(u)$ are both monotone and are equal at the end points. Then, the chord error is approximately kept within the give bound. Due to the initial conditions 11 of the seven-period profile, the speed function thus obtained is C^2 continuous.

If the maximal speed V_m is reached at certain critical point, the above algorithm does not use the full power of the machine. Let us explain this in detail. Suppose the $v_\mathrm{lim}(u_i) < V_\mathrm{m}$ and $v_\mathrm{lim}(u_{i+1}) > V_\mathrm{m}$ and there is a $u^* \in (u_i, u_{i+1})$ such that the limit speed at each point in $[u^*, u_{i+1}]$ is larger than V_m. Then the above algorithm cannot reach V_m at any point in $[u^*, u_{i+1})$. In general, to find u^* is computationally costs. A simple and improved idea is to use Algorithm **PRO_AD** instead of Algorithm **PRO_VV**. If $v_i < V_\mathrm{m}$ and $v_j = V_\mathrm{m}$, $j = i + 1, \ldots, i + s$, then Algorithm **PRO_AD** is used to interpolate $C(u), u \in [u_i, u_{i+s+1}]$. Notice that Algorithm **PRO_AD** will find an approximate value u^* after which the maximal speed V_m will be used.

Based on the above analysis, the following velocity planning algorithm with confined jounce is given.

After the velocity function is obtained, the parameter values of the interpolation points need to be computed. Suppose the curve segment to be interpolated is $C(u), u \in [u_1, u_2]$ and a velocity function $\bar{v}(t), t \in [0, t_\mathrm{m}]$ is obtained with Algorithm **VP_CJ**. Let T be the sampling period. Then the speed at the interpolation points can be obtained as $v_j = \max(\bar{v}(T \cdot j), 0.1)$ for $j = 0, 1, \ldots$. Note that we need to take 0.1 as the minimal interpolation velocity to ensure that the cutter can start to move at the beginning of a spline curve.

Suppose that the current parameter value is u_0 which corresponds to the interpolation speed v_j. To find the next parametric value $u_0 + \Delta u$, first compute the step size

$$\Delta L = v_j T \approx |C(u_0) C(u_0 + \Delta u)|,$$

where T is the sampling period. Because the interpolation distance ΔL in one period can be approximately treated as the arc length, the approximate relationship between two adjacent parameters about arc distance is [4, 16]

$$\Delta u = \frac{\Delta L}{\sigma(u_0)} - \frac{C'(u_0) \cdot C''(u_0) \Delta L^2}{2\sigma(u_0)^4} + o(\Delta L^2). \tag{25}$$

Since ΔL is a small quantity, from Eq. 25, we can compute Δu with the first-order Taylor approximation

$$\Delta u = \frac{\Delta L}{\sigma(u_0)} \tag{26}$$

or with the second-order Taylor approximation

$$\Delta u = \frac{\Delta L}{\sigma(u_0)} - \frac{D \Delta L^2}{2\sigma(u_0)^4} \tag{27}$$

where $D = (\frac{\mathrm{d}x}{\mathrm{d}u}\frac{\mathrm{d}^2x}{\mathrm{d}u^2} + \frac{\mathrm{d}y}{\mathrm{d}u}\frac{\mathrm{d}^2y}{\mathrm{d}u^2} + \frac{\mathrm{d}z}{\mathrm{d}u}\frac{\mathrm{d}^2z}{\mathrm{d}u^2})_{u=u_0}$. If the approximation fails, then use Newton's iterative method or the dichotomy to find $u_0 + \Delta u$.

Algorithm 3.4 VP_CJ($C(u), u \in [0, 1]$)

Input: B-spline curve $C(u), u \in [0, 1]$ as the tool path, the parameters S_m, J_m, A_m, V_m, T, and the chord error bound δ.

Output: A velocity function for the tool path, which satisfies the constraints.

1. $s = 1, u_1 = 0, k = 1$.
2. Use Algorithm **CR_PTS($C(u), u \in [0, 1]$)** to compute the critical points $\hat{u}_i, i = 1, \ldots, p$.
3. Use Algorithm **REACH($\hat{u}_i, i = 1, \ldots, p$)** to compute the reachable speeds $v_i, i = 1 \ldots, p$, at these points.
4. If $v_{k+1} < V_m$, go to step 5; else go to step 6.
5. Interpolation with Algorithm **PRO_VV**.
   (a) Use Algorithm **PRO_VV(v_k, v_{k+1})** to find (t_1, t_2, t_3).
   (b) Let $v_0(t)$ be the speed function in Eq. 31 determined with parameters (t_1, t_2, t_3), $t_m = 4t_1 + 2t_2 + t_3$, and d_m computed with Eq. 9. If $v_k \le v_{k+1}$, the velocity function is $v(t) = v_k + v_0(t)$; else the velocity function is $v(t) = v_k - v_0(t)$.
   (c) Let L be the length of the curve segment $C(u), u \in [u_k, u_{k+1}]$.
   (d) Let $\bar{t}_m = \frac{t_m L}{d_m}$ and set $\bar{v}(t) = v(\frac{t d_m}{L}), t \in [0, \bar{t}_m]$ to be the velocity function for the curve segment $C(u), u \in [u_k, u_{k+1}]$.
   (e) Set $k = k + 1$ and go to step 4.
6. Interpolation with Algorithm **PRO_AD**.
   (a) Let w be the largest number satisfying $v_{k+j} = V_m, j = 1, \ldots, w$.
   (b) Let L be the length of the curve segment $C(u), u \in [u_k, u_{k+w+1}]$.
   (c) Use Algorithm **PRO_AD(v_k, v_{k+w+1}, L)** to find $(t_1, t_2, t_3, t_4, t_5, t_6, t_7)$.
   (d) Let $d_c = (4t_1 + 2t_2 + t_3)(v_k + V_m)/2 + V_m t_4 + (4t_5 + 2t_6 + t_7)(v_{k+w+1} + V_m)/2$ be the distance of the AD profile from Eq. 19.
   (e) Let $v(t)$ be the speed function computed with Eq. 18 with parameters $(t_1, t_2, t_3, t_4, t_5, t_6, t_7)$.
   (f) Let $t_m = 4t_1 + 2t_2 + t_3 + t_4 + 4t_5 + 2t_6 + t_7$ and $\bar{t}_m = \frac{t_m L}{d_c}$. Set $\bar{v}(t) = v(\frac{d_c t}{L}), t \in [0, \bar{t}_m]$ to be the velocity function for the curve segment $C(u), u \in [u_k, u_{k+w+1}]$.
   (g) Set $k = k + w + 1$ and go to step 4.

Based on the above analysis, the following algorithm to compute the next interpolation point is given.

In most cases, formula 27 gives a nice approximation and the iterative methods are not needed.

Algorithm 3.5 NEXT_U($C(u), u_0, \Delta L$)

Input: B-spline curve $C(u)$ $u \in [0, 1]$, the current parameter u_0, and the next step size ΔL.

Output: The next interpolation parameter u_n.

1. Compute the second-order approximate Δu with Eq. 27.
2. If $\Delta u > 0$, set $u_n = u_0 + \Delta u$ and return u_n.
3. If $\Delta u < 0$, then use Newton iterative method to find the next parametric value.
   (a) Construct the following objective function in u
   $$f(u) = (x(u) - x(u_0))^2 + (y(u) - y(u_0))^2 + (z(u) - z(u_0))^2 - \Delta L^2.$$
   (b) Use Newton's iterative method to find the next interpolation parametric value with initial value $u = u_0 + \frac{\Delta L}{\sigma(u_0)}$ (first-order approximation)
   $$u^* = u - \frac{f(u)}{f'(u)}.$$
   (c) If $f(u^*) > \varepsilon$, $u^* < u_0$, or $u^* \gg u_0$, then the method fails, where ε is a given tiny positive number; otherwise, set $u_n = u^*$ and return u_n.
4. If the Newton method fails, then use the dichotomy to compute a solution u_n of $f(u) = 0$ in (u_0, u_r), where $u_r = u_0 + k\frac{\Delta L}{\sigma(u_0)}$ and k is the smallest natural number such that $f(u_r) > 0$. Return u_n.

Remark 3.6 The proposed method can be implemented in CNC controllers in the following way: Firstly, the velocity functions are computed off-line with Algorithm **VP_CJ**. Then the velocity functions are used as parts of the input to the CNC controllers to achieve real-time interpolation. Of course, the CNC controller must be modified to accept the new G codes. This strategy is adopted by many existing work such as [6, 18, 19, 21]. In particular, industrial CNC machining is realized in [18, 21] using this approach. The idea of the above approach is to use a pretreatment to add the velocity function to the G codes and then use the new G codes for CNC machining.

3.4 An illustrative example

An example is used to illustrate the algorithm. The tool path in Fig. 5a is a planar quadratic B-spline $(x(u), y(u)), u \in [0, 1]$ with C^1 continuity and consisting of six pieces of quadratic curve segments. Use the following parameters: $V_m = 50$ mm/s, $A_m = 1{,}500$ mm/s^2,

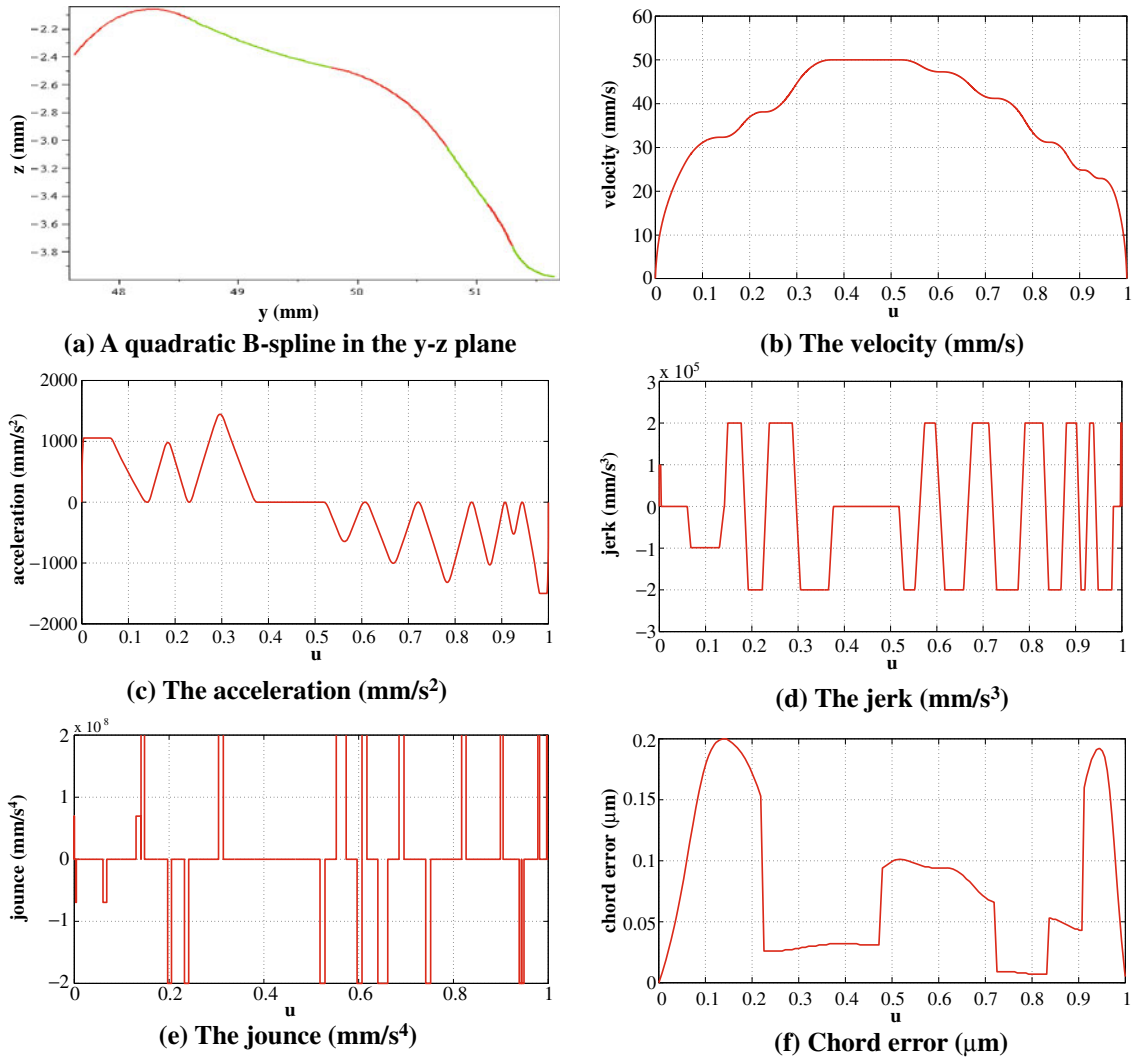

Fig. 5 Velocity, acceleration, jerk, jounce, and chord error functions of a quadratic spline. The *horizontal axis* is the parameter u for the tool path in **b**–**f**. **a** A quadratic B-spline in the y–z plane. **b** The velocity (millimeters per second). **c** The acceleration (millimeters per square second). **d** The jerk (millimeters per cubic second). **e** The jounce (millimeters per quartic second). **f** Chord error (micrometers)

$J_m = 2 \times 10^5$ mm/s^3, $S_m = 2 \times 10^8$ mm/s^4, $T = 1$ ms, and $\delta = 0.2$ μm.

Firstly, compute the critical points of the B-spline curve with Algorithm **CR_PTS**, and the parameter values u_i of the critical points are given in the first column of Table 1. The y- and z-coordinates of critical points are listed, respectively, in the second and third columns. $v_i = v_{\lim}(u_i)$ is listed in the fourth column. At $u = 0$, the velocity is set to be 0.1 mm/s to ensure that cutter can move at the beginning. In step 3, check the reachability of the limit speeds $v_{\lim}(u_i)$ at the critical points using Algorithm **REACH**, and the adjusted velocity is shown in the fifth column of Table 1. Note that the speeds at $u = 0.7208, 0.8354, 0.9069, 0.9438$ are obtained by the backtracking step of Algorithm **REACH** due to the final speed at $u = 1.0$.

The speed function obtained is shown in Fig. 5b. Its acceleration, jerk, and jounce are shown in Fig. 5c–e, respectively. From Fig. 5b–e, it is not difficult to see that either the jounce, jerk, acceleration, or the velocity reaches their maximal values except in $I_1 = [0, 0.1407]$. By the results proved in Section 3, this means that the velocity is time-optimal except in I_1. In the parameter interval I_1, the tool path length L is larger than the length d_m of the seven-period profile to increase the speed from zero to the limit speed at $u = 0.1407$ in step 6(d) of Algorithm **VP_CJ**. As a consequence, the velocity function over I_1 is not time optimal. Figure 5f gives the theoretic chord error under the planned velocity and the sampling period T, which is less than the given bound δ for all parameter values.

Table 1 Information of critical points (unit for speed: millimeters per second)

u_i	$y(u_i)$ (mm)	$z(u_i)$ (mm)	v_i	Adjusted v_i
0	47.62	−2.39	49.654	0.1
0.1407	48.2112	−2.06188	32.3387	32.3387
0.2303	48.6154	−2.13848	93.2816	38.124
0.4017	49.4231	−2.40066	91.7538	50
0.4724	49.7656	−2.47271	92.0354	50
0.6071	50.3573	−2.69218	47.2607	47.2607
0.7208	50.7513	−3.04704	140.729	41.2157
0.8354	51.1049	−3.46825	48.4228	31.1962
0.9069	51.3000	−3.75227	51.5066	24.8385
0.9438	51.4077	−3.88634	23.9501	22.9357
1.0000	51.66	−3.98	31.4245	0.1

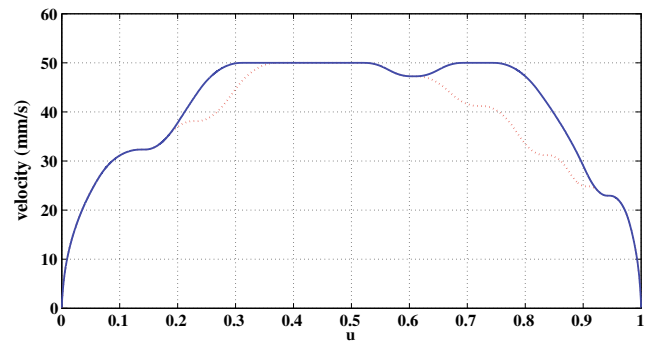

Fig. 6 *Red one* velocity function of Algorithm 3.4. *Blue one* velocity function of the improved method

The velocity of the key point given by Algorithm **REACH** can be improved. Before doing the reachability test, delete some useless key points according to whether its velocity is constrained by the others. Precisely, if the velocity of parameter u_i is $v(u_i)$, then from this point, under a given length l, the velocity is limited. So use an acceleration profile from the start point $(u_i, v(u_i))$, with $j(u_i) = a(u_i) = 0$, from a forward velocity function $v^+(t)$ or $v^+(u)$. Check whether $v^+(u_{i+1}) < v(u_{i+1})$. If $v^+(u_{i+1}) < v(u_{i+1})$ and $v^+(u_{i+1}) < V_{\mathrm{m}}$, then the key point $(u_{i+1}, v(u_{i+1}))$ can be deleted since the final velocity at u_{i+1} will never exceed $v(u_{i+1})$. Finally, use the renewed key points to do the velocity planning.

By this improved method, the selected critical points and new velocities are given in Table 2. The key points $u = 0.2303$, $u = 0.8354$, and $u = 0.9069$ are deleted according to the above rule. The velocity functions of the improved method and Algorithm 3.4 are given in Fig. 6, which shows that the velocity function obtained with the improved method is better than the previous one.

4 Experimental results

In this section, experimental results will be presented. The first experiment shows that confined jounce indeed can be used to reduce vibration of the CNC machine tools. The second experiment shows the feasibility of the interpolation method by simulating two real CNC machining models.

4.1 Vibration test

In this section, we will compare three AD profiles with confined acceleration, confined jerk, and confined jounce in a CNC machine to show that confined jounce indeed can be used to reduce vibration comparing to confined jerk and acceleration.

The equipment used to test vibration is LMS SCADAS3 which is a fast signal acquisition and analysis system, including hardware and software components. The hardware component consists of sensors, exciters, data acquisition tools, and a laptop PC. The software component can be used for real-time signal acquisition, calculation, analysis, display, record, and

Table 2 Information of critical points with the improved method (unit for speed: millimeters per second)

u_i	$y(u_i)$ (mm)	$z(u_i)$ (mm)	v_i	Selected or deleted	Adjusted v_i
0	47.62	−2.39	49.654	Selected	0.1
0.1407	48.2112	−2.06188	32.3387	Selected	32.3387
0.2303	48.6154	−2.13848	93.2816	Deleted	–
0.4017	49.4231	−2.40066	91.7538	Selected	50
0.4724	49.7656	−2.47271	92.0354	Selected	50
0.6071	50.3573	−2.69218	47.2607	Selected	47.2607
0.7208	50.7513	−3.04704	140.729	Selected	50
0.8354	51.1049	−3.46825	48.4228	Deleted	–
0.9069	51.3000	−3.75227	51.5066	Deleted	–
0.9438	51.4077	−3.88634	23.9501	Selected	22.9357
1.0000	51.66	−3.98	31.4245	Selected	0.1

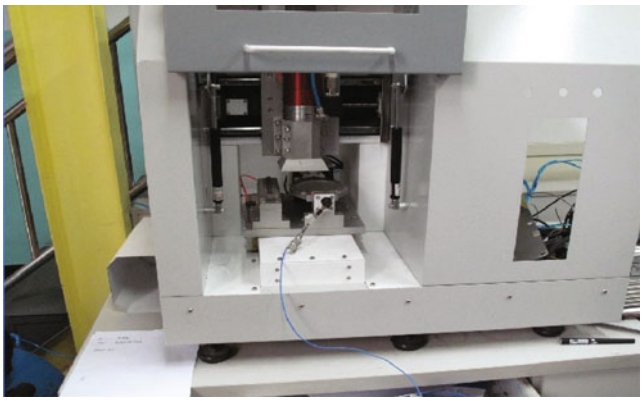

Fig. 7 The CNC machine and the sensor attached on the machine

output. Figure 7 shows the LMS SCADAS3 sensor attached to a CNC machine.

In the vibration test, the tool path is a line segment of 100 mm, and the CNC machine tool will idly move along the line segment. Three AD profiles are used, respectively, to generate the velocity function: the linear AD profile with confined acceleration, the S-spate AD profile with confined jerk, and the AD profile with confined jounce introduced in this paper. The maximal speed V_m, acceleration A_m, jerk J_m, jounce S_m, and the machining time t are given in Table 3. The three velocity functions are shown in the right-hand side of Fig. 8.

The sampling time of LMS SCADAS3 is 1 s, and the sampling frequency is 4,096 Hz. Since the machining time is about 2 s, we record the signals from machining the first half of the line segment only. The vibration frequency spectrum diagrams of the three tests are given in the left-hand side of Fig. 8, where the vertical axis is the vibration intensity whose unit is grams per hertz and g is the gravitational acceleration, and the unit of horizontal axis is hertz. The spectrum diagram gives the distribution of the intensity of the vibration at difference frequencies. For instance, from Fig. 8a, the strongest vibration with intensity 0.016 g/Hz occurs when the machine tool vibrates at frequency 980 Hz.

From Fig. 8, one can see that for confined acceleration, the maximal vibration is 0.016 g/Hz, and the machine vibrates relatively strong (>0.004 g/Hz) in the frequency intervals [0, 200] and [820, 1,450]. For confined jerk, the maximal vibration is 0.0145 g/Hz, and the machine vibrates relatively strong (>0.004 g/Hz) in the frequency intervals [0, 180] and [850, 1,430]. For confined jerk, the maximal vibration is 0.008 g/Hz, and the machine vibrates relatively strong (>0.004 g/Hz) in the frequency intervals [0, 180] and [870, 1,220]. It is very clear that in the case of confined jerk, the machine vibrates significantly less than that of confined acceleration, and in the case of confined jounce, the machine vibrates significantly less than that of confined jerk.

From Table 3, the machining times for confined acceleration, confined jerk, and confined jounce are 2.051, 2.101, 2.201 s, respectively. Comparing to the confined acceleration and confined jerk, the machining time with confined jounce increases about 7.3% and 4.8%, respectively.

In summary, using confined jounce, with the loss of not much machining time, we can reduce the vibration significantly comparing with confined acceleration and confined jerk. It is known that the machining quality is affected by many factors, and vibration of the machining tool is certainly one of the important factors. We choose to test vibration instead of machining quality directly for the following reason: By running the CNC machine tool idle, the affect of the adopted AD profile on the vibration becomes more significant and from which we can see more clearly the difference of the three AD profiles.

4.2 Simulation results on two CNC machining models

In this section, simulation results on two CNC machining models will be presented to show the feasibility of the interpolation algorithm. All the computations are carried out using C language on a PC with Windows XP, a 2.13-GHz CPU, and 1.98-GB memory.

The first model is the "vase" shown in Fig. 9a. The vase is a CNC model consisting of more than 116,000 G01 codes with total tool path length of 46.67 m. Its B-spline representation consists of more than 42,000 quadratic curve segments [21]. The G01 codes and the spline representation of the model can be found in http://www.mmrc.iss.ac.cn/~xgao/cnc/vase.html. The tool path of the vase fluctuates violently making optimal speed velocity planning difficult. The spline curve in Fig. 5 is from this model.

The second model is one piece of blade in the "impeller" shown in Fig. 9b, which is a cubic B-spline with C^2 continuity and consisting of 394 cubic curve

Table 3 Parameters of tests (a), (b), (c) and the interpolation time

Test	S_m (mm/s^4)	J_m (mm/s^3)	A_m (mm/s^2)	V_m (mm/s)	d (mm)	t (s)
(a)	–	–	1,000	50	100	2.051
(b)	–	20,000	1,000	50	100	2.101
(c)	200,000	20,000	1,000	50	100	2.201

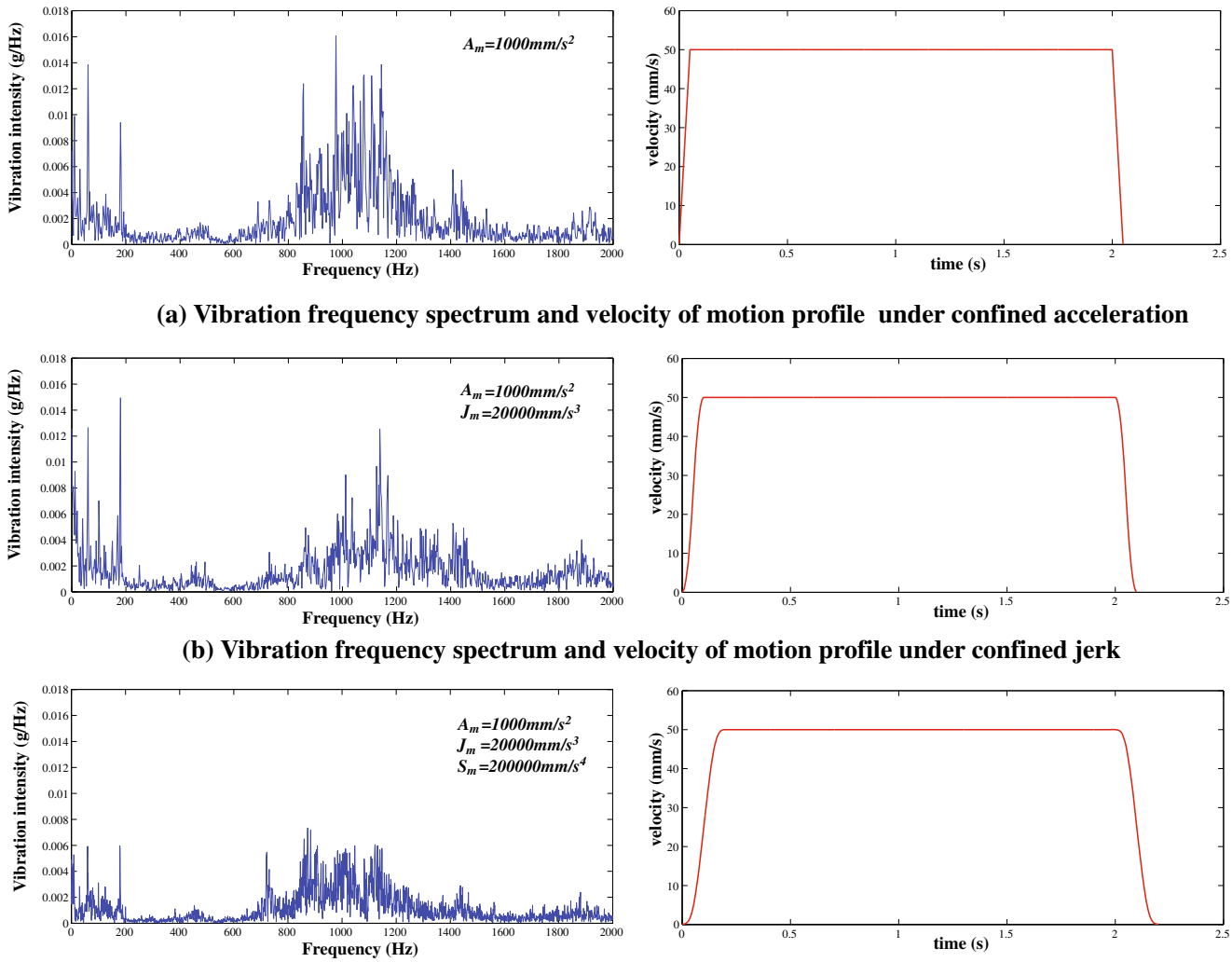

Fig. 8 The vibration frequency spectrum diagrams and the corresponding velocity functions. **a** Vibration frequency spectrum and velocity of motion profile under confined acceleration. **b** Vibration frequency spectrum and velocity of motion profile under confined jerk. **c** Vibration frequency spectrum and velocity of motion profile under confined jounce

segments [21]. The total tool path length of the blade is 3.167 m. The G01 codes and the spline representation of the model can be found in http://www.mmrc.iss.ac.cn/~xgao/cnc/blade.html. Note that this is a five-axis model: $(x(u), y(u), z(u), A(u), C(u))\ u \in [0, 1]$. For simplicity, the velocity for the (x, y, z) tool path is planned with the method introduced in this paper and the parameter values u_i thus obtained are used to compute the angular interpolation positions $(A(u_i), C(u_i))$.

In both experiments, the following parameters are used: $V_\mathrm{m} = 200$ mm/s, $T = 1$ ms, $\delta = 0.2$ μm, and S_m, J_m and A_m are taken different values for comparison, which are shown in Table 4. Note that in our method, the speed decreases to zero at the connection points of two splines. This could be further improved using the method given in [7].

Tables 4 and 5 give the machining timings for the "vase" model and the "impeller" model under different bounds of acceleration, jerk, and jounce. Tables 6 and 7 give the times needed to compute the velocity function and the interpolation points for the "vase" and "impeller" models, respectively. In Tables 6 and 7, "t_V" and "t_P" denote the times to compute the velocity function and the interpolation points, respectively.

From Tables 6 and 7, we can see that the computation time of the algorithm is much less than the machining time. As mentioned in Remark 3.6, the velocity function is computed off-line and the interpolation points are computed in real time. For the "vase" model and the "impeller" model, the times to compute the interpolation point are 13–18% and 5–8% of the machining times, indicating that the algorithm is feasible for real-time implementation.

(a) The vase model **(b) The impeller model**

Fig. 9 Two CNC machining models. **a** The vase model. **b** The impeller model

Table 4 The machining times of "vase" model under different constraints

A_m	$J_m = 5 \times 10^5$ mm/s^3		$J_m = 2 \times 10^5$ mm/s^3	
(mm/s^2)	$S_m = 2 \times 10^8$ (min)	$S_m = 1 \times 10^8$ (min)	$S_m = 2 \times 10^8$ (min)	$S_m = 1 \times 10^8$ (min)
1,000	25.1167	26.3298	26.4793	27.2322
2,000	22.3648	23.5293	24.0420	24.8345
3,000	21.4223	23.1568	23.4963	24.2998
6,000	20.7693	22.5608	23.2368	24.0440

The unit for S_m is millimeters per quartic second

Table 5 The machining time of "impeller" model under different constraints

A_m	$J_m = 5 \times 10^5$ mm/s^3		$J_m = 2 \times 10^5$ mm/s^3	
(mm/s^2)	$S_m = 2 \times 10^8$ (min)	$S_m = 1 \times 10^8$ (min)	$S_m = 2 \times 10^8$ (min)	$S_m = 1 \times 10^8$ (min)
1,000	0.5757	0.5816	0.5830	0.5856
2,000	0.4583	0.4647	0.4704	0.4759
3,000	0.3982	0.4153	0.4259	0.4297
6,000	0.3549	0.3650	0.3997	0.4037

The unit for S_m is millimeters per quartic second

Table 6 Time to compute velocity functions (t_V) and interpolation points (t_P) for "vase" model

A_m	$J_m = 5 \times 10^5$ mm/s^3				$J_m = 2 \times 10^5$ mm/s^3			
(mm/s^2)	$S_m = 2 \times 10^8$		$S_m = 1 \times 10^8$		$S_m = 2 \times 10^8$		$S_m = 1 \times 10^8$	
	t_V (s)	t_P (s)	t_V (s)	t_P (s)	t_V (s)	t_P (s)	t_V (s)	t_P (s)
1,000	117.06	205.42	119.03	207.40	120.59	210.21	120.37	211.36
2,000	131.98	207.93	135.73	208.08	136.08	209.04	141.16	217.21
3,000	139.59	204.47	143.06	209.28	142.20	210.98	143.45	210.13
6,000	143.34	204.05	147.91	208.89	142.57	206.69	147.32	211.80

The unit for S_m is millimeters per quartic second

Table 7 Time to compute velocity functions (t_V) and interpolation points (t_P) for "impeller" model

A_m	$J_m = 5 \times 10^5$ mm/s^3				$J_m = 2 \times 10^5$mm/s^3			
(mm/s^2)	$S_m = 2 \times 10^8$		$S_m = 1 \times 10^8$		$S_m = 2 \times 10^8$		$S_m = 1 \times 10^8$	
	t_V (s)	t_P (s)	t_V (s)	t_P (s)	t_V (s)	t_P (s)	t_V (s)	t_P (s)
1,000	0.594	1.844	0.609	1.813	0.690	1.716	0.638	1.800
2,000	0.702	1.735	0.595	1.827	0.598	1.855	0.530	1.907
3,000	0.658	1.779	0.671	1.767	0.629	1.855	0.592	1.876
6,000	0.577	1.798	0.595	1.795	0.549	1.888	0.591	1.877

The unit for S_m is millimeters per quartic second

5 Conclusion

In this paper, an acceleration/deceleration profile with confined jounce, jerk, acceleration, and speed is designed, and its properties are studied. In particular, it is shown that the profile is time optimal to change the speed from one value to another under the given constraints. Based on the jounce confined acceleration/deceleration profile, an interpolation method for parametric tool paths is given. The idea is to compute the maximal speeds at the critical points of the tool path where the radius of curvature reaches extremal values and to use the jounce confined acceleration/deceleration profile to connect the speeds of two adjacent critical points. The final velocity function has C^2 continuity. A vibration test is given to show that comparing with confined acceleration and jerk, the motion profile under confined jounce can reduce vibration more effectively.

In most existing work on interpolation, the friction force and the cutting force in Eq. 1 are assumed to be independent of the velocity. An interesting problem is to plan the velocity by assuming the existence of certain relation between the cutting force and the velocity. Another problem is to plan the velocity under confined chord error and confined jounce in each axis as done in [14, 18, 19] in simpler cases such as confined acceleration or confined jerk.

Acknowledgments The authors are grateful to Prof. Peiqing Ye from Tsinghua University, who provided the equipments for the vibration test reported in Section 4.1. This study was partially supported by a National Key Basic Research Project of China (2011CB302400) and by a grant from NSFC (60821002).

Appendix

In this appendix, the seven-period acceleration profile and the proof of its time-optimal property are given.

Formulas for the seven-period acceleration profile

Assume that initial velocity $v_s = 0$. The following formulas are the expressions of the jounce $s(t)$, jerk $j(t)$, acceleration $a(t)$, and speed $v(t)$, $t \in [0, t_m]$ for the seven-period acceleration profile in Fig. 1.

$$s(t) = \begin{cases} S_m, & 0 \le t < t_1, \\ 0, & t_1 \le t < t_1 + t_2, \\ -S_m, & t_1 + d_2 \le t < 2t_1 + t_2, \\ 0, & 2t_1 + t_2 \le t < 2t_1 + t_2 + t_3, \\ -S_m, & 2t_1 + t_2 + t_3 \le t < 3t_1 + t_2 + t_3, \\ 0, & 3t_1 + t_2 + t_3 \le t < 3t_1 + 2t_2 + t_3, \\ S_m, & 3t_1 + 2t_2 + t_3 \le t < 4t_1 + 2t_2 + t_3 \end{cases} \tag{28}$$

$$j(t) = \begin{cases} S_m t, & 0 \le t < t_1, \\ S_m t_1, & t_1 \le t < t_1 + t_2, \\ S_m(2t_1 + t_2 - t), & t_1 + t_2 \le t < 2t_1 + t_2, \\ 0, & 2t_1 + t_2 \le t < 2t_1 + t_2 + t_3, \\ S_m(2t_1 + t_2 + t_3 - t), & 2t_1 + t_2 + t_3 \le t < 3t_1 + t_2 + t_3, \\ -S_m t_1, & 3t_1 + t_2 + t_3 \le t < 3t_1 + 2t_2 + t_3, \\ S_m(t - 4t_1 - 2t_2 - t_3), & 3t_1 + 2t_2 + t_3 \le t < 4t_1 + 2t_2 + t_3 \end{cases} \tag{29}$$

$$a(t) = \begin{cases} \frac{1}{2} S_m t^2, & 0 \le t < t_1, \\ S_m t_1 t - \frac{1}{2} S_m t_1^2, & t_1 \le t < t_1 + t_2, \\ -\frac{1}{2} S_m (2t_1 + t_2 - t)^2 + S_m(t_1 t_2 + t_1^2), & t_1 + t_2 \le t < 2t_1 + t_2, \\ S_m(t_1 t_2 + t_1^2), & 2t_1 + t_2 \le t < 2t_1 + t_2 + t_3, \\ S_m(t_1 t_2 + t_1^2) - \frac{1}{2} S_m (2t_1 + t_2 + t_3 - t)^2, & 2t_1 + t_2 + t_3 \le t < 3t_1 + t_2 + t_3, \\ 2S_m t_1 t_2 + \frac{7}{2} S_m t_1^2 + S_m t_1 t_3 - S_m t_1 t, & 3t_1 + t_2 + t_3 \le t < 3t_1 + 2t_2 + t_3, \\ \frac{1}{2} S_m (t - 4t_1 - 2t_2 - t_3)^2, & 3t_1 + 2t_2 + t_3 \le t < 4t_1 + 2t_2 + t_3 \end{cases} \tag{30}$$

$$
v_0(t) = \begin{cases}
\frac{1}{6}S_m t^3, & 0 \le t < t_1, \\
\frac{1}{2}(t-t_1)^2 S_m t_1 + \frac{1}{2}(t-t_1)S_m t_1^2 + \frac{1}{6}S_m t_1^3, & t_1 \le t < t_1 + t_2, \\
\frac{1}{3}S_m t_1^3 + \frac{1}{2}S_m t_1^2 t_2 - S_m t_1^2 t + \frac{1}{2}S_m t_1 t_2^2 - S_m t_1 t_2 t & \\
+S_m t_1 t^2 + \frac{1}{6}S_m t_2^3 - \frac{1}{2}S_m t_2^2 t + \frac{1}{2}S_m t_2 t^2 - \frac{1}{6}S_m t^3, & t_1 + t_2 \le t < 2t_1 + t_2, \\
-S_m t_1^3 - \frac{3}{2}S_m t_1^2 t_2 - \frac{1}{2}S_m t_1 t_2^2 + S_m t_1 t_2 t + S_m t_1^2 t, & \\
& 2t_1 + t_2 \le t < 2t_1 + t_2 + t_3, \\
S_m(t_1 t_2 + t_1^2)(t - 2t_1 - t_2 - t_3) + \frac{1}{6}S_m(2t_1 + t_2 + t_3 - t)^3 & \\
+S_m t_1^3 + \frac{3}{2}S_m t_1^2 t_2 + \frac{1}{2}S_m t_1 t_2^2 + S_m t_1 t_2 t_3 + S_m t_1^2 t_3, & \\
& 2t_1 + t_2 + t_3 \le t < 3t_1 + t_2 + t_3, \\
2S_m t_1 t_2 t + \frac{7}{2}S_m t_1^2 t + S_m t_1 t_3 t - \frac{1}{2}S_m t_1 t^2 - 4S_m t_1^2 t_2 & \\
-S_m t_1 t_2^3 - S_m t_1 t_2 t_3 - \frac{25}{6}S_m t_1^3 - \frac{5}{2}S_m t_1^2 t_3 - \frac{1}{2}S_m t_1 t_3^2, & \\
& 3t_1 + t_2 + t_3 \le t < 3t_1 + 2t_2 + t_3, \\
-\frac{26}{3}S_m t_1^3 + 4S_m t_1 t_3 t - 7S_m t_1 t_2 t_3 + 8S_m t_1 t_2 t + 2S_m t_2 t_3 t & \\
-7S_m t_1 t_2^2 + 8S_m t_1^2 t - 2S_m t_1 t^2 - 13S_m t_1^2 t_2 - 7S_m t_1^2 t_3 & \\
-2S_m t_1 t_3^2 - S_m t_2 t^2 - \frac{1}{2}S_m t_3 t^2 + 2S_m t_2^2 t + \frac{1}{2}S_m t_3^2 t & \\
-2S_m t_2^2 t_3 - S_m t_2 t_3^2 + \frac{1}{6}S_m t^3 - \frac{4}{3}S_m t_2^3 - \frac{1}{6}S_m t_3^3 & \\
& 3t_1 + 2t_2 + t_3 \le t < 4t_1 + 2t_2 + t_3 \\
2S_m t_1^3 + S_m t_1 t_2 t_3 + S_m t_1 t_2^2 + 3S_m t_1^2 t_2 + S_m t_1^2 t_3, & 4t_1 + 2t_2 + t_3 \le t.
\end{cases} \tag{31}
$$

Proof for Theorem 2.3

In order to prove Theorem 2.3, the following result is needed.

Theorem A.1 (Birkhoff and Rota [1], pp. 24–26) *Let y, z be solutions of the following differential equations*

$$y' = F(x, y), z' = G(x, z),$$

respectively, where $F(x, y) \le G(x, y), a \le x \le b$, and F or G satisfies Lipschitz's condition. If $y(a) = z(a)$, then $y(x) \le z(x)$ for any $x \in [a, b]$.

Proof of Theorem 2.3 First of all, prove the seven-period jerk profile is time optimal. Denote by $v(t), t \in [0, t_m]$ the velocity curve of the seven-period jerk profile, where $t_m = 4 * t_1 + 2 * t_2 + t_3$, and denote by $j(t), a(t)$ its corresponding jerk and acceleration. Claim that for any other velocity curve $v^*(t), t \in [0, t^*]$ which satisfies the constraints 10 and 11, $t^* \ge t_m$. Also, denote by $j^*(t), a^*(t), s^*(t)$ the jerk and acceleration and jounce of $v^*(t)$, respectively. Assume on the contrary, there exists a $t_4 \in [0, t^*]$, such that $v(t_4) < v^*(t_4)$ (especially take $t_4 = t^*$). Show that this t_4 does not exist for $t_4 \in [0, t_m]$.

Case 1, $t_4 \notin [0, t_1 + t_2]$. Since for $t \in [0, t_1 + t_2]$, $j(t) \ge j^*(t)$, then $a(t) \ge a^*(t)$ and $v(t) \ge v^*(t)$.

Case 2, $t_4 \notin (t_1 + t_2, 2 * t_1 + t_2]$. If this is not the case, then there exists a $t_5 \in (t_1 + t_2, t_4]$ such that $a(t_5) < a^*(t_5)$. Claim that $j(t_5) \le j^*(t_5)$. If this is not the case, that is $j(t_5) > j^*(t_5)$. Then, by Theorem A.1, $j(t) = j(t_5) + \int_t^{t_5} S_m \mathrm{d}t_s > j^*(t) + \int_t^{t_5} s^*(t_s)\mathrm{d}t_s = j^*(t)$ for $t \in [t_1 + t_2, t_5]$. Then $a(t_5) < a^*(t_5)$ is impossible by case 1. Let $t_6 = 2 * t_1 + t_2 - t_5$, then by Theorem A.1, $j^*(t) = j^*(t_5) - \int_{t_5}^{t} s^*(t_s)\mathrm{d}t_s \ge j(t)$, for $t \in [t_5, t_5 + t_6]$. Then, by Theorem A.1,

$$
\begin{aligned}
a^*(t_5 + t_6) &= a^*(t_5) + \int_{t_5}^{t_5+t_6} j^*(t)\mathrm{d}t \\
&\ge a^*(t_5) + \int_{t_5}^{t_5+t_6} j(t)\mathrm{d}t \\
&> a(t_5) + \int_{t_5}^{t_5+t_6} j(t)\mathrm{d}t \\
&> A_m
\end{aligned}
$$

This contradicts to the constraint 10.

Case 3, $t_4 \notin (2 * t_1 + t_2, 2 * t_1 + t_2 + t_3]$. If this is not the case, there exists a $t_5 \in [0, 2 * t_1 + t_2)$ such that $a(t_5) < a^*(t_5)$. This is impossible by the discussion in cases 1 and 2.

Case 4, $t_4 \notin (2 * t_1 + t_2 + t_3, t_m)$. Denote $\bar{v}^*(t)$ by

$$
\bar{v}^*(t) = \begin{cases} 0, & t \in [0, t_m - t^*) \\ v^*(t + t^* - t_m), & t \in [t_m - t^*, t_m] \end{cases}
$$

Similar to the cases 1, 2, 3, for $t \in [2*t_1+t_2, t_m]$, from the $-t$ direction, $v(t)$ uses the extremal deceleration capability to decrease its velocity. So, $v(t) \le \bar{v}^*(t), t \in [2*t_1+t_2, t_m]$. Since $v(t)$ is monotone, let $t_5 = 2*t_1+t_2+t^*-t_m \in [0, 2*t_1+t_2]$, then $v(t_5) < v(t_5+t_m-t^*) \le \bar{v}^*(t_5+t_m-t^*) = v^*(t_5)$. This contradicts to cases 1 and 2.

The time-optimal properties of other type acceleration profile can be proved in a similar way by adding the different constraints. So far, it has been proved that Algorithm **PRO_VV** is a time-optimal procedure to increase the speed from v_s to v_e under the constraints 10 and 11.

It needs to be proved that the selections of concrete jerk profiles given in Section 2 are reasonable. For simplicity, consider only the transitions from $(+,+,+)$ to $(+,+,-)$ or $(+,-,+)$ and from $(+,+,-)$ to $(+,-,-)$ or $(+,-,+)$. Without loss of generality, let $v_s = 0$.

First, it is obvious to find that $(+,+,+)$ is the most optimal profile if feasible. But on condition of $J_m^2 < S_m A_m$, if $v_e < \frac{A_m^2}{J_m} + \frac{A_m J_m}{S_m}$, then v_e is not large enough for profile $(+,+,+)$ and the profile transition should be considered. If profile $(+,-,+)$ is adopted, then $t_2 = 0$ and $t_3 > 0$, $j_m \le J_m < \sqrt{S_m A_m}$.

Obviously $t_1 = \frac{j_m}{S_m}$. By Eq. 8, v_e is of the following form:

$$v_e = 2S_m t_1^3 + S_m t_1 t_2 t_3 + S_m t_1 t_2^2 + 3S_m t_1^2 t_2 + S_m t_1^2 t_3$$
$$= 2S_m t_1^3 + S_m t_1^2 t_3,$$

so $t_3 = \frac{v_e S_m}{j_m^2} - \frac{2j_m}{S_m}$ and the time of profile $(+,-,+)$ is $t_{(+,-,+)} = t(j_m) = \frac{v_e S_m}{j_m^2} + \frac{2j_m}{S_m}$. So according to the value of v_e, when $v_e < \frac{A_m^2}{J_m} + \frac{A_m J_m}{S_m}$, there are two cases to be discussed.

Case a: $v_e > \frac{2J_m^3}{S_m^2}$. Since $t(j_m)$ is monotonically decreasing on interval $j_m \in (0, (v_e S_m^2)^{\frac{1}{3}}]$ and $j_m \le J_m < (\frac{v_e S_m^2}{2})^{\frac{1}{3}}$, $t(j_m) \ge \frac{v_e S_m}{J_m^2} + \frac{2J_m}{S_m}$. It is easy to find that $\frac{v_e S_m}{J_m^2} + \frac{2J_m}{S_m} > \frac{J_m}{S_m} + \sqrt{\frac{J_m^2}{S_m^2} + \frac{4v_e}{J_m}} = t_{(+,+,-)}$. So $t_{(+,-,+)} > t_{(+,+,-)}$. The time of profile $(+,+,-)$ is less than that of profile $(+,-,+)$.

Case b: $v_e \le \frac{2J_m^3}{S_m^2}$. In this case, profile $(+,+,-)$ is invalid; otherwise, j_m exceeds J_m. Now show that the time of profile $(+,-,-)$ is less than that of profile $(+,-,+)$. If profile $(+,-,+)$ is adopted, then $t_1 = \frac{j_m}{S_m}$ and $t_2 = 0$ and $t_3 = \frac{v_e S_m}{j_m^2} - \frac{2j_m}{S_m} > 0$. So $j_m < (\frac{v_e S_m^2}{2})^{\frac{1}{3}}$. Denote by $t(j_m) = 4*t_1+t_3$ the total acceleration time with maximal jerk j_m. Since $t(j_m)$ is monotonically decreasing on interval $j_m \in (0, (v_e S_m^2)^{\frac{1}{3}}]$, $t_{(+,-,+)} = t(j_m) > t((\frac{v_e S_m^2}{2})^{\frac{1}{3}}) = 4(\frac{v_e}{2S_m})^{\frac{1}{3}} = t_{(+,-,-)}$. So the time of profile $(+,-,-)$ is less than that of profile $(+,-,+)$.

Thus, the optimality of profile transition in Algorithm **PRO_VV** has been proved. Other cases can be proved similarly. Now Theorem 2.3 is proved. □

If the acceleration profile is symmetric, then time optimal means the distance to accelerate v_s to v_e is the shortest one since the distance is $d = \frac{v_s+v_e}{2}t^*$, where t^* is the total acceleration time.

References

1. Birkhoff G, Rota G (1969) Ordinary differential equations. Blaisdell, New York
2. Bobrow J-E, Dubowsky S, Gibson J-S (1985) Time-optimal control of robotic manipulators along specified paths. Int J Rob Res 4(3):3–17
3. Erkorkmaz K, Altintas Y (2001) High speed CNC system design. Part I: jerk limited trajectory generation and quintic spline interpolation. Int J Mach Tools Manuf 41:1323–1345
4. Farouki RT, Tsai YF (2001) Exact Taylor series coefficients for variable-feedrate CNC curve interpolators. CAD 33(2):155–165
5. Gai R, Lin H, Zheng L, Huang Y (2009) Design and implementation of velocity planning algorithm for high speed machining (in Chinese). Journal for Chinese Computer Systems 30(6):1067–1071
6. Lai J-Y, Lin K-Y, Tseng S-J, Ueng W-D (2008) On the development of a parametric interpolator with confined chord error, feedrate, acceleration and jerk. Int J Adv Manuf Technol 37:104C121
7. Lee A-C, Lin M-T, Pana Y-R, Lin W-Y (2011) The feedrate scheduling of NURBS interpolator for CNC machine tools. CAD 43:612C628
8. Li Y-Y, Feng J-C, Wang Y-h, Yang J-G (2009) Variable-period feed interpolation algorithm for high-speed five-axis machining. Int J Adv Manuf Technol 40:769–775
9. Macfarlane S, Croft E-A (2003) Jerk-bounded manipulator trajectory planning: design for real-time applications. IEEE Trans Robot Autom 19:42–52
10. Nam S-H, Yang N-Y (2004) A study on a generalized parametric interpolator with real-time jerk-limited acceleration. Comput Aided Des 36:27–36
11. Park J, Nam S-H, Yang M-Y (2005) Development of a real-time trajectory generator for NURBS interpolation based on the two-stage interpolation method. Int J Adv Manuf Technol 26:359–365
12. Schellekensa P, Rosiellea N, Vermeulena H, Vermeulena M, Wetzelsa S, Prila W (2008) Design for precision: current status and trends. CIRP J Manuf Syst 47(2):557–586
13. Shiller Z (1994) On singular time-optimal control along specified paths. IEEE Trans Robot Autom 10:561–566

14. Timar S-D, Farouki R-T (2007) Time-optimal traversal of curved paths by Cartesian CNC machines under both constant and speed-dependent axis acceleration bounds. Robot Comput-Integr Manuf 23(5):563–579
15. Wang J-B, Yau H-T (2008) Real-time NURBS interpolator: application to short linear segments. Int J Adv Manuf Technol 41:1169–1185
16. Xu Z-M, Chen J-C, Feng Z-J (2002) Performance evaluation of a real-time interpolation algorithm for NURBS curves. Int J Adv Manuf Technol 20:270–276
17. Yong T, Narayanaswami R (2003) A parametric interpolator with confined chord errors, acceleration and deceleration for NC machining. CAD 35:1249–1259
18. Yuan C-M, Zhang K, Fan W, Gao X-S (2011) Time-optimal interpolation for CNC machining along curved tool paths with confined chord error. MM Res Preprints 30:57–89
19. Zhang K, Gao X-S, Li H, Yuan C-M (2010) A greedy algorithm for feedrate planning of CNC machines along curved tool paths with jerk constraints. MM Res Preprints 29:189–205
20. Zhang L-X, Sun R-Y, Gao X-S, Li H-B (2011) High speed interpolation for micro-line trajectory and adaptive real-time look-ahead in CNC machining. Sci China E 54(6):1481–1495
21. Zhang M, Yan W, Yuan C-M, Wang D-K, Gao X-S (2011) Curve fitting and optimal interpolation on CNC machines based on quadratic B-splines. Sci China F 54(7):1407–1418